Sustainable Energy & Fuels

Photoredox system with biocatalyst for CO_2 utilization

Journal:	*Sustainable Energy & Fuels*
Manuscript ID	SE-REV-05-2018-000209.R1
Article Type:	Review Article
Date Submitted by the Author:	11-Jun-2018
Complete List of Authors:	Amao, Yutaka; Osaka City University, Advanced Research Institute for Natural Science and Technology; Osaka City University, Research Center for Artificial Photosynthesis

Journal Name

ARTICLE

Photoredox system with biocatalyst for CO_2 utilization

Y. Amao[a,b]*

Received 00th January 20xx,
Accepted 00th January 20xx

DOI: 10.1039/x0xx00000x

www.rsc.org/

Various researches on visible-light driven redox systems for hydrogen production, CO_2 reduction and utilization are paid much attention to the solar fuel and chemical production. In general, the visible-light driven redox system is consisted of an electron donor, a photocatalytic dye, an electron mediator and a catalyst. One of the important component in the visible-light driven redox system is effective catalyst for hydrogen production, CO_2 reduction and utilization. The catalyst used in the visible-light driven redox system is classified into metal nanoparticles, molecular catalyst and biocatalyst. Among these catalysts, the biocatalyst is one of promising catalyst because it has excellent selectivity of the reaction and substrate. For CO_2 reduction and utilization, especially, the highly reaction selectivity of the biocatalyst is remarkable in comparison with other various catalysts. Among biocatalysts for CO_2 reduction and utilization, $NAD(P)^+$-dependent dehydrogenases that are commercially available are widely used for the visible-light driven redox system of CO_2 reduction. Formate dehydrogenase (FDH) from *Candida boidinii* is typical $NAD(P)^+$-dependent dehydrogenase for the visible-light driven redox of CO_2 reduction to formate. Furthermore, by adding commercially available aldehyde (aldDH), formaldehyde (FldDH) and alcohol dehydrogenase (ADH) to this system, CO_2 is reduced to methanol via the formate and formaldehyde as the intermediators in the visible-light driven redox system. Among biocatalysts for CO_2 reduction and utilization, in contrast, $NAD(P)^+$-dependent dehydrogenases with the function of decarboxylating that also are commercially available are widely used for the visible-light driven building carbon-carbon bond from CO_2 and organic molecule. Malic enzyme (ME) from Chicken liver is typical $NAD(P)^+$-dependent dehydrogenase with decarboxylating for the visible-light driven malate production based on the building carbon-carbon bond from CO_2 and pyruvate. In this review, the visible-light driven CO_2 reduction and utilization systems consisted of photoreduction of $NAD(P)^+$ and biocatalysts are introduced. Furthermore, the visible-light driven CO_2 reduction and utilization systems consisted of photoreduction of bipyridinium salt (viologen)-based electron mediator and biocatalysts also are introduced. In particular, by utilizing the viologen-based electron mediator, the simplification of the visible-light driven CO_2 reduction and utilization systems and the improvement of efficiency without changing the structure of the biocatalyst also are mentioned.

Introduction

Greenhouse gases are chemical compounds, which induce the greenhouse effect. The rapidly increase in Earth's atmospheric concentrations of the three main human-made greenhouse gases –CO_2, methane, and nitrous oxide– is clear from the data sets for these gases over the last 400,000 years. Among these greenhouse gasses, CO_2 is the most important greenhouse gas produced by human activities, primarily through the combustion of fossil fuels. Its concentration in the Earth's atmosphere has risen by more than 30% since the Industrial Revolution. Thus, the development of technology for CO_2 gas reduction drastically is important for the future.[1] The protocol concerning the CO_2 reduction in the atmosphere is deliberated at the Kyoto Conference on Climate Change (COP3).[2] Furthermore, at the 2009 U.N. Summit on Climate Change held at New York, Prime Minister of Japan at that time declared, "Japan administration would aim to cut greenhouse gas emissions more than 25% by 2020 from 1990 levels". Recently, the Paris climate accord (COP21) is an agreement dealing with greenhouse gas emissions mitigation, adaptation, and finance starting in the year 2020. The COP21 is negotiated in Paris and adopted by consensus on 12 December 2015. CO_2 needs to be drastically reduced (more than 30%) worldwide from 2030 to 2050.[3] Thus, the production of low-carbon fuels, hydrogen, CO_2 based alcohol and so on by using renewable energy such as solar energy is important for mitigating global warming. As the examples of hydrogen production, CO_2 reduction and utilization using solar energy, various visible-light driven redox systems consisting of a photocatalytic dye and catalyst are paid much attention to the solar fuel and chemical production. In general, the visible-light driven redox system is consisted of an electron donor (D), a photocatalytic dye (P), an electron mediator (C) and a catalyst as shown in Fig 1.[4-10]

[a] Advanced Research Institute for Natural Science and Technology, Osaka City University, Sugimoto 3-3-138, Sumiyoshi-ku, Osaka 558-8585, Japan
[b] Research Center for Artificial Photosynthesis, Osaka City University, Sugimoto 3-3-138, Sumiyoshi-ku, Osaka 558-8585, Japan
[c] See DOI: 10.1039/x0xx00000x

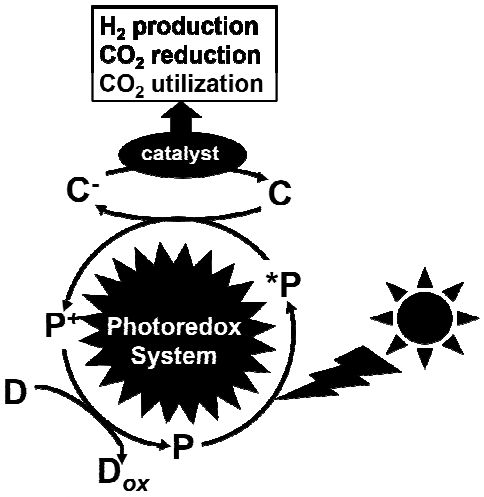

Fig. 1. Scheme of the visible-light driven redox system consisted of an electron donor (D), a photocatalytic dye (P), an electron mediator (C) and a catalyst.

One of the important component in this system is effective catalyst for hydrogen production, CO_2 reduction and utilization. The catalyst used in this system is classified into metal nanoparticles, molecular catalyst and biocatalyst. For example of catalyst for hydrogen production, platinum nanoparticle,[11-21] cobalt,[23-26] platinum,[27-33] or iron-based molecular catalyst [34-44] is used as catalyst in the visible-light driven hydrogen production with a photocatalytic dye. Biocatalyst, hydrogenase (H_2ase) [45-53] also is used as catalyst in the visible-light driven hydrogen production. Studies using H_2ase as a catalyst for visible-light driven hydrogen production systems with various photocatalytic dye, ruthenium polypyridyl coordinate complexes, metaloporphyrins, semiconductors based metal oxide and so on, have been conducted from the 1970s to today.[54-66]

For example of catalyst for CO_2 reduction and utilization, in contrast, copper-based catalyst,[67-76] silver-loaded metal oxide,[77-82] rhenium or iron-based molecular catalyst[83-90] is used as catalyst in the visible-light driven CO_2 reduction to CO, formate and so on with a photocatalytic dye. Problems with using these catalysts for the visible-light driven CO_2 reduction are low selectivity of products, simultaneous hydrogen production and so on. By using copper-based catalyst for CO_2 reduction and utilization in the electrochemical reaction, CO, formate, methane, ethylene, ethanol, *n*-propanol and hydrogen production are observed. The copper-based catalyst with gallium nitride based semiconductor is applied to the light-driven CO_2 reduction as an example.[91] In this system, the solar energy conversion yield is estimated to be 0.2 %. However, products based on CO_2 reduction are CO, formate, methane, ethylene, ethanol and so on. As the CO_2 reduction selectivity for products is low, thus, it is difficult to obtain the desired products based on the CO_2 reduction in this system.

Visible-light driven CO_2 reduction systems have been studied using cobalt polypyridyl or macrocyclic complexes and rhenium bipyridyl complexes. Visible-light driven CO_2 reduction to CO have been accomplished using rhenium bipyridyl complex. In this system, simultaneous hydrogen production is observed. A system consisting of triethylamine (TEA) as an electron donor, tris(2-phenylpyridinato)iridium(III) ($Ir(ppy)_3$) as a photocatalytic dye, Fe(III)-porphyrin based catalyst (chloro iron(III) 5,10,15,20-tetra(40-*N,N,N*-trimethylanilinium) porphyrin; Fe-*p*-TMA, chloro iron(III) 5,10,15,20-tetrakis(2',6'-dihydroxyphenyl) porphyrin; Fe-*o*-OH or chloro iron(III) tetraphyneylporphyrin; FeTPP) for visible-light driven CO_2 reduction to methane with high selectivity has also been reported.[92] In this system, CO, methane and hydrogen are produced with the visible-light irradiation (> 420 nm). By using Fe-*p*-TMA as a catalyst for CO_2 reduction, CO is the main product for the direct CO_2 photoreduction, however, a two-pot procedure that first reduces CO_2 and then reduces CO converts methane with a selectivity of up to 82 % and a quantum yield of 0.18 % as an example. The proposed mechanism for the visible-light driven CO_2 reduction to methane with Fe(III) porphyrin-based catalyst is as follows. At first, the Fe(III) porphyrin-based catalyst is reduced with 3-electrons to the catalytically produced Fe(0) active species. The Fe (0) species reduces CO_2, with the resultant Fe(I) regenerated through electron transfer from the photoexcited $Ir(ppy)_3$. The CO produced binds to Fe (II) and is further reduced with a total of 6-electrons, transferred from the photoexcited $Ir(ppy)_3$ and 6-protons to generate methane, via a Fe(I)-formyl as a proposed intermediate. Some studies on the light driven CO_2 reduction with silver nanoparticle-loaded gallium oxide are reported. In this system, CO_2 reduction to CO and simultaneous hydrogen production are observed. A system consisting of a semiconductor photocatalyst, bismuth vanadium oxide ($BiVO_4$) and a cobalt(II) chlorin (Co(II) Chl) based molecular catalyst for the visible-light driven CO_2 reduction to CO with high selectivity has also been reported. In this system, a surface-modified $BiVO_4$ onto fluorine-doped tin oxide (FTO) photoanode with iron(III) oxide(hydroxide), FeO(OH) (FeO(OH)/$BiVO_4$ /FTO) and a Co(II) Chl as a cathode active material adsorbed on multiwalled carbon nanotubes (Co(II) Chl - modified cathode) are used. Photoelectrochemical CO_2 reduction occurs using this system, to produce CO with 83% Faradaic efficiency at an applied bias voltage of − 1.3 V at the Co(II) Chl - modified cathode vs the FeO(OH)/$BiVO_4$ /FTO photoanode under visible light irradiation in a CO_2 -saturated aqueous solution (pH 4.6). The difference in the oxidation potential of the FeO(OH)/BiVO4 /FTO electrode under dark and that under visible-light irradiation is estimated to be *ca.* 1.5 V, which is smaller than that of band gap of $BiVO_4$ (band gap energy: 2.4 eV), indicating that the FeO(OH)/$BiVO_4$ /FTO photoanode lowers the total bias that enables simultaneous water oxidation and CO_2 reduction to CO.[93] From these research results, it is an important task to improve the selectivity of CO_2 photoreduction products using metal-based, molecular catalyst and photocatalyst.

Among these catalysts for CO_2 reduction and utilization, the biocatalyst is one of promising catalyst because it has excellent selectivity of the reaction and substrate in homogenous aqueous media. Organic molecules syntheses based on the biocatalytic methods have been much paid attention because of their regio- and stereo-selectivity, and mild physiological conditions. Biocatalytic syntheses compete with conventional methods based on the chemical synthesis, especially in organic molecules syntheses that are not able to be successfully carried out by chemical catalysts. Examples of beneficial biocatalytic reactions are oxidations of alkanes, alkenes, and aromatics.[94] As the biocatalytic reactions proceed in aqueous solution as a reaction medium, moreover, the biocatalytic methods are attractive for green process in the chemistry of CO_2 reduction and utilization.

For example, formate dehydrogenase (FDH) catalyzes the oxidation and reduction between formate and CO_2 with the redox coupling NAD^+/NADH as a co-enzyme. Thus, visible-light driven CO_2 reduction to formate will be developed with the photoredox systems as shown in Fig. 1 consisting of an electron donor, a photocatalytic dye, and an electron mediator in the presence of FDH as a catalyst.

Biocatalysts for CO_2 reduction and utilization are classified into two categories: 1) CO_2 reduction to CO or formate, 2) building carbon-carbon bond from CO_2 and organic molecule to produce carboxylic acid. Carbon monoxide dehydrogenase (CODH) and FDH are biocatalysts for CO_2 reduction to CO and formate, respectively. The system consisting of FDH, aldehyde dehydrogenase (AldDH) and alcohol dehydrogenase (ADH) is used for the CO_2 reduction to methanol via formate and formaldehyde as an intermediator.

Malic enzyme (ME) and isocitrate dehydrogenase (IDH) are biocatalysts for building carbon-carbon bond from CO_2 and pyruvate and 2-oxoglutarate to produce malate and isocitrate, respectively.

In the visible-light driven CO_2 reduction and utilization, photocatalytic dyes with high visible-light sensitization activity are desired to act as model for the natural photosynthetic dye such as chlorophyll. The model compounds used as photosynthetic dyes are classified mainly into four categories.[95] The first category comprises of porphyrin compounds. The second category is ruthenium polypyridyl complexes. The third category is of natural photosynthesis dyes, such as chlorophyll and its derivatives. The fourth category is photocatalytic material such as CdS, TiO_2 and so on.

The electron mediators for the visible-light driven CO_2 reduction and utilization with the biocatalysts are easily reduced with a photocatalytic dye and need to function as a co-enzyme for biocatalysts. $NAD(P)^+$, bipyridinium salts (so-called viologen) and rhodium complexes are widely used as the electron mediator in the visible-light driven CO_2 reduction and utilization with the biocatalysts. The photocatalytic dye (P), the electron mediator (C) and the biocatalyst utilized in the visible-light driven CO_2 reduction and utilization are summarized in Fig. 2.

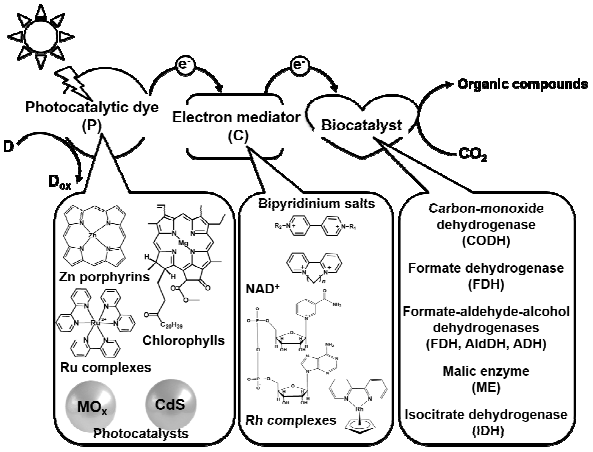

Fig. 2. Summary of the photocatalytic dye (P), the electron mediator (C) and the biocatalyst utilized in the visible-light driven CO_2 reduction and utilization.

In this review, the properties of commercially available biocatalysts for CO_2 reduction and utilization are introduced. The visible-light driven CO_2 reduction and utilization systems consisted of photoreduction of $NAD(P)^+$ and biocatalysts are introduced. Furthermore, the visible-light driven CO_2 reduction and utilization systems consisted of photoreduction of viologen-based electron mediator and biocatalysts also are introduced. In particular, by utilizing the viologen-based electron mediator,[96] the simplification of the visible-light driven CO_2 reduction and utilization systems and the improvement of efficiency without changing the structure of the biocatalyst also are mentioned.

Biocatalysts for CO_2 reduction and utilization

Biocatalysts for CO_2 reduction

Biocatalysts with the function of CO_2 reduction for the light driven redox systems are introduced in this section. Biocatalyst for the light driven CO_2 reduction is a set of enzyme that catalyze the oxidation of C_1 materials such as formate, CO and so on to CO_2, donating the electrons to a second substrate $NAD(P)^+$ and the reverse reaction of CO_2 reduction, donating the electrons to a second substrate NAD(P)H. These biocatalysts are so-called to $NAD(P)^+$-dependent dehydrogenases. Typical $NAD(P)^+$-dependent dehydrogenases for CO_2 reduction are shown in Fig. 3.

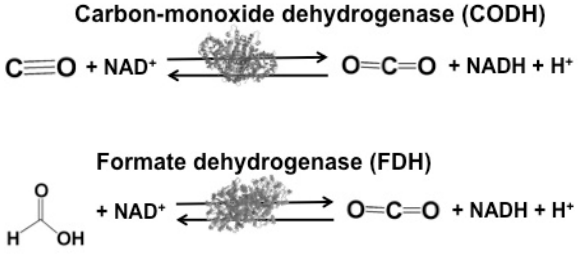

Fig. 3. Reaction schemes of biocatalysts carbon-monoxide (CODH) and formate (FDH) dehydrogenases.

Biocatalysts for the CO_2 reduction to CO and formic acid are carbon-monoxide dehydrogenase (CODH)[97-101] and formate dehydrogenase (FDH),[102-105] respectively. Especially, FDH obtained from *Candida boiidini* (EC 1.2.1.2), that are commercially available biocatalyst, is widely used for various CO_2 reduction systems to formic acid using light driven redox, photoelectrochemical and thermal catalytic reaction.

The CO_2 reduction to methanol, that is paid attention to a low-carbon alcohol fuel, is developed with the combination of FDH, commercially available aldehyde (AldDH)[106-108] from *Yeast* (EC 1.2.1.5) and alcohol dehydrogenase (ADH)[109,110] from *Yeast* (EC 1.1.1.1). AldDH catalyzes the oxidation of formaldehyde to formic acid in the presence of $NAD(P)^+$ and the reverse reaction of formic acid to formaldehyde in the presence of NAD(P)H. ADH catalyzes the oxidation of methanol to formaldehyde in the presence of $NAD(P)^+$ and the reverse reaction of formaldehyde to methanol in the presence of NAD(P)H.

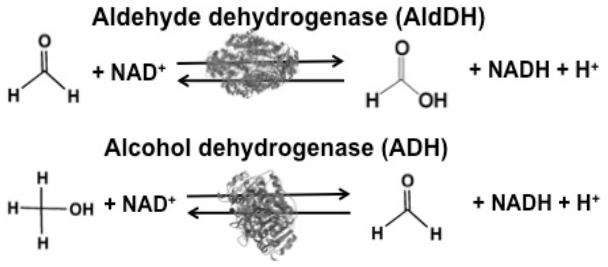

Fig. 4. Reaction schemes of biocatalysts aldehyde (AldDH) and alcohol (ADH) dehydrogenases.

By using shared co-enzyme, NAD(P)H for FDH, FldDH and ADH, CO_2 reduction to methanol via formate and formaldehyde as the intermediates is developed as shown in Fig. 5.

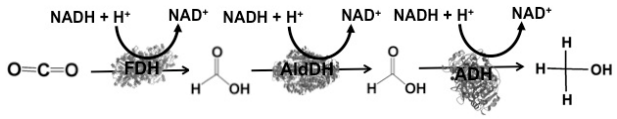

Fig. 5. Reaction scheme of CO_2 reduction to methanol with FDH, FldDH, and ADH in the presence of NADH.

For example, the CO_2 reduction to methanol in FDH, FldDH, and ADH immobilized silica sol-gel matrices have been accomplished in the presence of NADH. The yield of NADH to methanol is estimated to be 21.0 % in the solution system, in contrast to 91.2 % using the silica sol-gel system.[111] The CO_2 reduction to methanol by using FDH, FldDH, and ADH immobilized onto polystyrene particle has also been developed with glutamate dehydrogenase (GluDH) for utilization of redox coupling NAD^+/NADH. In the solution system, the yield of CO_2 reduction to methanol is estimated to be 12%, while it is estimated to be 80% using biocatalysts co-immobilized polystyrene particle system. [112]

Formaldehyde dehydrogenase (FldDH) from *Pseudomonas sp.* (EC 1.2.1.46) specialized for formaldehyde oxidation and formate reduction with the redox coupling NAD^+/NADH is also commercially available.

The visible-light driven CO_2 reduction can be developed by combining a photoreduction of NAD^+ to NADH and a biocatalyst such as FDH, the complex system of FDH, FldDH and ADH.

Biocatalysts for CO_2 utilization

Biocatalysts with the function of CO_2 utilization based on building carbon-carbon bond for the light driven redox systems are introduced in this section. Biocatalysts for the CO_2 utilization with the light driven redox system is a set of enzyme that catalyze the decarboxylation or carboxylation with redox coupling $NADP^+$/NADPH. Malic enzyme (ME) [113-118] and isocitrate dehydrogenase (IDH)[119-122] are typical biocatalysts for the CO_2 utilization as shown in Fig. 6.

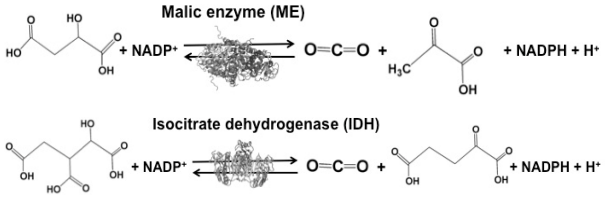

Fig. 6. Reaction schemes of biocatalysts malic enzyme (ME) and isocitrate dehydrogenase (IDH).

ME from *Chicken liver* (EC 1.1.1.40) and IDH from *Yeast* (EC 1.1.1.41) are commercially available biocatalysts. ME catalyzes the reaction of malate conversion to pyruvate and CO_2, and the reverse reaction of pyruvate and CO_2 conversion to malate using redox coupling $NADP^+$/NADPH. IDH catalyzes the reaction of isocitrate conversion to 2-oxoglutarate and CO_2, and the reverse reaction of 2-oxoglutarate and CO_2 conversion to isocitrate using redox coupling $NADP^+$/NADPH.

For example, the pyruvate and CO_2 conversion to malate by using ME has also been developed[121,122] with glucose-6-phosphate dehydrogenase for utilization of redox coupling $NADP^+$/NADPH. Under optimal conditions using this system, the ratio of CO_2 and pyruvate to malate is estimated to be about 38 % after 24 h of incubation.[121]

The visible-light driven CO_2 utilization based on building carbon-carbon bond can be developed by combining a photoreduction of $NADP^+$ to NADPH and a biocatalyst such as ME and IDH.

Photoredox system for light driven CO_2 reduction

Photoredox system for light driven CO_2 reduction with biocatalyst via the redox couple of $NAD(P)^+$/ NAD(P)H

To use a FDH or the complex system of FDH, AldDH and ADH as a CO_2 reduction catalyst, in a simple idea, these biocatalysts are applied to a visible-light driven redox system of NAD^+/NADH. For example, visible-light driven CO_2 reduction to formate will be developed with the redox system consisting of an electron donor (D), a photocatalytic dye (P), and NAD^+ in the presence of FDH, as shown in Fig. 7.

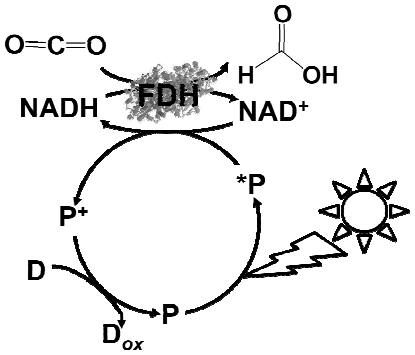

Fig. 7. Scheme of the visible-light driven redox system for CO_2 reduction to formate consisted of an electron donor (D), a photocatalytic dye (P), NAD^+ and FDH.

However, the NAD dimer, $(NAD)_2$ forms in the reaction of the single-electron reduced NAD^+ with a photocatalytic dye, such as tris(bipyridine)ruthenium(II) $(Ru(bpy)_3^{2+})$, as shown in Fig. 8. Moreover, the reaction between NAD^+ and $(NAD)_2$ is irreversible process.[123-127] As $(NAD)_2$ is an inactive co-enzyme for NAD^+-dependent dehydrogenase such as FDH, AldDH, ADH and so on, it is difficult to achieve the photoredox system based on the combination of NAD^+ photoreduction and FDH for the CO_2 reduction to formate.

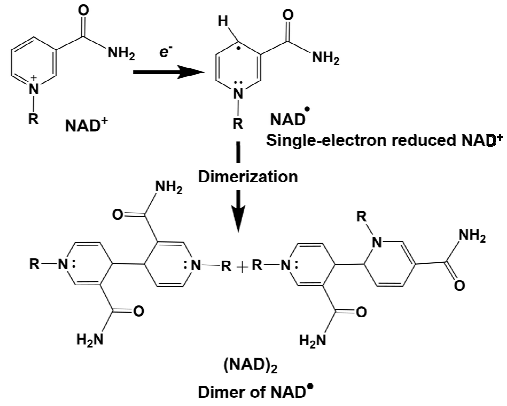

Fig. 8. Dimerization process of the single-electron reduced NAD^+ ($NAD^•$).

In contrast, some studies on the visible-light driven reduction of NAD^+ to NADH by a photocatalytic dye via the second catalyst, such as rhodium complex, ferredoxin-$NADP^+$ reductase (FNR) (EC 1.18.12) and so on, have been reported. In this system, for example, NAD^+ dimerization is suppressed via the iridium or rhodium complex.

The NAD^+ reduction to NADH with iridium complex, Ir (III) (Cp*)(4-(1*H*–pyrazol-1-yl-κN^2)benzoate-κC^3)$(H_2O)^+$ (Cp*: 1,2,3,4, 5-pentamethylcyclopenta-dienyl) is introduced as an example. [128] Redox process of iridium complex, Ir (III) (Cp*)(4-(1*H* -pyrazol-1-yl-κN^2)benzoate-κC^3)$(H_2O)^+$ is shown in Fig. 9.

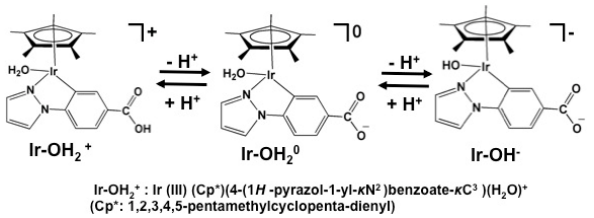

Fig. 9. Redox process of iridium complex, Ir (Cp*)(4-(1*H* -pyrazol-1-yl-κN^2)benzoate-κC^3)$(H_2O)^+$ (Cp*: 1,2,3,4,5-pentamethylcyclopentadienyl)

The hydrogen gas induced NAD^+ reduction to NADH proceeds with redox coupling of iridium complex as shown in Fig. 10. In this process, the iridium hydride complex ($Ir\text{-}OH^-$) produced under an atmospheric pressure of hydrogen gas undergoes the 1,4-selective hydrogenation of NAD^+ to form NADH.

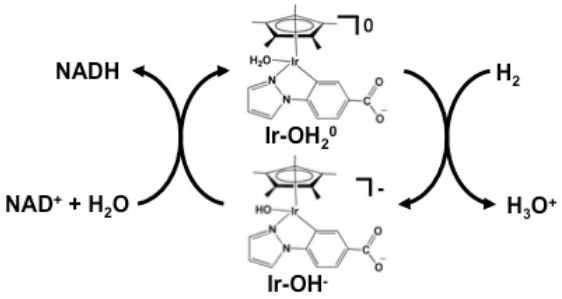

Fig. 10. The process of NAD^+ reduction to NADH with iridium complex and hydrogen gas.

Visible-light driven NAD^+ reduction to NADH with the system of a photocatalytic dye and rhodium complex, $Cp^*Rh(bpy)(OH_2)^{2+}$ as an electron mediator is developed as shown in Fig. 11.[129-132]

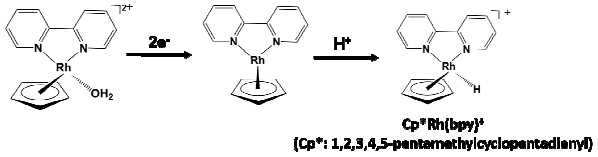

Fig. 11. Redox process of rhodium complex, $Cp^*Rh(bpy)(OH_2)^{2+}$

Carbon-doped TiO_2, boron doped TiO_2, multianthraquinone-substituted porphyrin (MAQSP) with the chemically converted graphene (CCG) (MAQSP/CCG) and so on are used as a photocatalytic dye in a $Cp^*Rh(bpy)\ (OH_2)^{2+}$ electron-mediated NAD^+ reduction to NADH. The conversion yields of NAD^+ to NADH for carbon-doped TiO_2, boron-doped TiO_2, MAQSP/CCG, MAQSP, and $W_2Fe_4Ta_2O_{17}$ in this system are estimated to be 94.2, 94.0, 44.5, 23.8 and 14.5 % (2 h irradiation), respectively. [131] The conversion yields of NAD^+ to NADH using the

trisubstitution of isatin onto porphyrin ring provided 1,1',1''-((20-(2-((7-amino-9,10-dioxo-9,10-dihydroanthracen-2-yl) amino)quinolin-3-yl) porphyrin-5,10,15-triyl) tris (quinoline-3,2-diyl)) tris(indoline-2,3-dione) (IP) with the CCG (IP/CCG) and IP as the photocatalytic dye in this system are estimated to be 38.9 and 7.03 % (90 min irradiation), respectively. [132]

Table 1 shows the summary of conversion yields of NAD^+ to NADH in the light driven redox system of a photocatalytic dye and Cp*Rh(bpy) $(OH_2)^{2+}$.

Table 1. The conversion yields of NAD^+ to NADH in the light driven redox system of a photocatalytic dye and Cp*Rh(bpy) $(OH_2)^{2+}$.

Photocatalytic dye	Conversion yields of NAD^+ to NADH (%)	Reference
Carbon-doped TiO_2	94.2	129
Boron-doped TiO_2	94.0	130
MAQSP/CCG	44.5	132
MAQSP	23.8	132
$W_2Fe_4Ta_2O_{17}$	14.5	132
IP/CCG	38.9 (90 min irradiation)	133
IP	7.03 (90 min irradiation)	133

By using the Cp*Rh(bpy) $(OH_2)^{2+}$ as an electron mediator, light driven NAD^+ reduction system to NADH is developed with a photocatalytic dye. By using MAQSP/CCG as a photocatalytic dye in this system, visible-light driven CO_2 reduction to formate proceeds with FDH as a catalyst also is accomplished as shown in Fig. 12. In this system, $W_2Fe_4Ta_2O_{17}$ and MAQSP also are used as the photocatalytic dyes.[132]

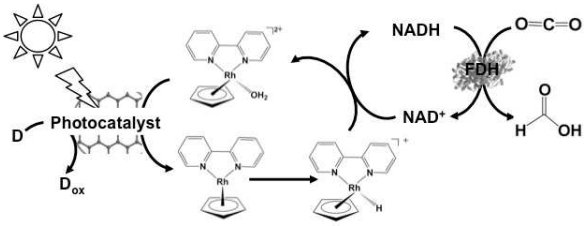

Fig. 12. Scheme of the visible-light driven redox system for CO_2 reduction to formate consisted of an electron donor (D), a photocatalyst, Cp*Rh(bpy) $(OH_2)^{2+}$, NAD^+ and FDH.

Typical reaction condition is composed of photocatalytic dye (0.5 mg), NAD^+ (1.24 µmol), rhodium complex (0.62 µmol), and FDH (3 units) in 3.1 mL of sodium phosphate buffer (100 mM, pH 7.0) with TEOA (1.24 mmol) in the presence of CO_2. The efficiency of formate production in the system of MAQSP/CCG, Cp*Rh(bpy), NAD^+ and FDH is 110.55 µmol after 2 h irradiation, while the systems using $W_2Fe_4Ta_2O_{17}$ and MAQSP are 14.25 and 46.53 µmol, respectively.[132]

Table 2 shows the summary of formate production after 2 h irradiation in the light driven CO_2 reduction system of a photocatalytic dye and Cp*Rh(bpy) $(OH_2)^{2+}$ via the NAD^+/NADH redox coupling with FDH.

Table 2. Formate production in the light driven CO_2 reduction system of a photocatalytic dye and Cp*Rh(bpy) $(OH_2)^{2+}$ via the NAD^+/NADH redox coupling with FDH.

Photocatalytic dye	Formate production (µmol)	Reference
MAQSP/CCG	110.55	132
MAQSP	46.53	132
$W_2Fe_4Ta_2O_{17}$	14.25	132

The other the visible-light driven redox system for CO_2 reduction to formate is consisted of an electron donor (D), a photocatalyst, Cp*Rh(bpy) $(OH_2)^{2+}$, NAD^+ and FDH, chemically converted graphene (CCG) covalently bonded to a light harvesting BODIPY molecule (1-picolylamine-2-aminophenyl-3-oxyphenyl-4,40-difluoro-1,3,5,7-tetr-amethyl-2,6-diethyl-4-bora-3a,4adiaza-*s*-indacene-triazine) (CCG-BODIP) is used as a photocatalytic dye.[134]

The photocatalyst-biocatalyst coupled system developed using CCG–BODIPY as photocatalyst functions, leading to NADH regeneration with about 54 %, followed by its consumption in about 144 µmol of formate production from CO_2.

As the visible-light driven redox system for CO_2 reduction to formate is consisted of an electron donor (D), a photocatalyst, Cp*Rh(bpy) $(OH_2)^{2+}$, NAD^+ and FDH is accomplished, methanol production is developed by adding FldDH and ADH in this system as shown in Fig. 13. In this system, IP/CCG, MAQSP/CCG and IP are used as the photocatalytic dyes.[132]

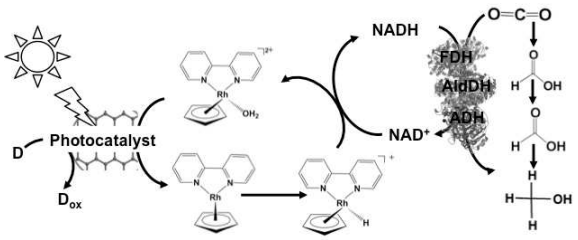

Fig. 13. Scheme of the visible-light driven redox system for CO_2 reduction to methanol consisted of an electron donor (D), a photocatalyst, Cp*Rh(bpy) $(OH_2)^{2+}$, NAD^+, FDH, FldDH and ADH.

Typical reaction condition is composed of photocatalytic dye (0.5 mg), NAD^+ (1.24 µmol), rhodium complex (0.62 µmol), FDH (9 units), FldDH (9 units) and ADH (9 units) in 3.1 mL of sodium phosphate buffer (100 mM, pH 7.0) with TEOA (1.24 mmol) in the presence of CO_2.

The methanol concentration in the system using IP/CCG as a photocatalytic dye is estimated to be 11.21 µM after 1 h visible-light irradiation. On the other hand, only 5.62 µM of methanol concentration is obtained with CCGCMAQSP as a photocatalytic dye. Moreover, no methanol production is observed in the system using IP as a photocatalytic dye. From these results, the CO_2 reduction yield with the system of a photocatalytic dye, Cp*Rh(bpy) $(OH_2)^{2+}$, NAD^+ and biocatalyst depends on the efficiency of NAD^+ reduction to NADH.

Table 3 shows the summary of methanol production after 1 h irradiation in the light driven CO_2 reduction system of a

photocatalytic dye and Cp*Rh(bpy) $(OH_2)^{2+}$ via the NAD^+/NADH redox coupling with FDH, FldDH and ADH.

Table 3. Methanol production in the light driven CO_2 reduction system of a photocatalytic dye and Cp*Rh(bpy) $(OH_2)^{2+}$ via the NAD^+/NADH redox coupling with FDH, FldDH and ADH.

Photocatalytic dye	Methanol production (μM)	Reference
IP/CCG	11.21	133
IP	5.62	133

A semi - biological light driven CO_2 reduction to formate system combining reduction of $NADP^+$ with photosynthetic protein and FDH has also been constructed. For example, light driven CO_2 reduction to formate by photosynthetic protein Cyanobacterial Photosystem I (PSI) and NADPH-dependent FDH via the $NADP^+$/NADPH redox coupling has been reported as shown in Fig. 12. In this system, $NADP^+$ reduction to NADPH with FNR via the redox protein, ferredoxin (Fd) is used as show in Fig. 14.[135]

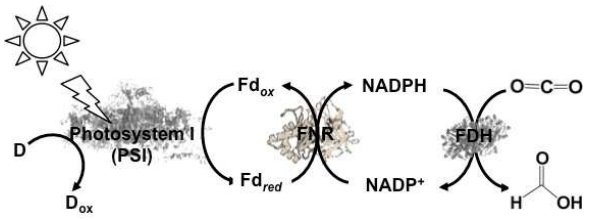

Fig. 14. Scheme of the visible-light driven redox system for CO_2 reduction to formate consisted of an electron donor (D), PSI as a photocatalytic material, Fd, FNR, $NADP^+$ and FDH.

In this system, FDH from *Pseudomonas sp*. 101 (EC 1.2.1.2) mutant (PsFDH[QN]) are used as a biocatalyst for CO_2 reduction. Typical reaction condition for light driven CO_2 reduction to formate production is performed in 3 mL phosphate buffer by using PS I at a concentration of 100 μg chlorophyll/mL, 10 mM ascorbate, 10 μM plastocyanin (PC), 2 μM Fd, 0.5 μM FNR, 1 mM $NADP^+$, 4 mM NADPH, 56 μM PsFDH[QN], 0.05% Triton X-100, and 10% sucrose. In this system, PC acts as an electron donor. The formate concentration linearly increased with irradiation time after about a 30 min lag time. The maximum rate of formate production is estimated to be 26 μM h^{-1}. In the reaction under a 10% O_2 and 90% CO_2 gas saturated condition, no formate is detected, indicating the O_2-sensitivity of the system. In addition, this study introduced the NADPH-dependent FDH mutant into heterocysts of the cyanobacterium *Anabaena sp.* PCC 7120 and demonstrated an increased formate concentration in the whole cells. These results provide a new possibility for visible-light driven CO_2 reduction.

With a new concept for $NADP^+$ reduction, amino group-modified dendrimer (Den-NH_2) is used as an electron mediator for $NADP^+$ reduction to NADPH in the visible-light driven redox system. For example, the visible-light driven CO_2 reduction to methanol with the combination of FDH, FldDH and ADH and $NADP^+$ reduction to NADHP with the system of a photocatalytic dye and Den-NH_2 as an electron mediator is also developed as shown in Fig. 15.[136]

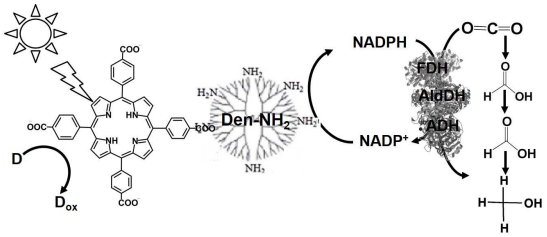

Fig. 15. Scheme of the visible-light driven redox system for CO_2 reduction to methanol consisted of an electron donor (D), tetrakis(4-carboxyphenyl)porphyrin (TCCP) as a photocatalytic dye, Den-NH_2, $NADP^+$, FDH, FldDH and ADH.

In this system, attempts are made to improve the reaction efficiency by adsorbing CO_2, $NADP^+$ or NADPH, FDH, FldDH and ADH to a Den-NH_2. For CO_2 reduction to methanol, TCPP, Den-NH_2, FDH, FldDH, ADH and NADPH are immobilized onto organoclay-incorporated 2,2,6,6-tetramethylpiperidine-1-oxyl (TEMPO)-oxidized cellulose nanofiber (TOCNF) films (Den-TCPP-NADPH (FDH/FldDH/ADH)-TOCNF). By using Den-TCPP-NADPH (FDH/FldDH/ADH)-TOCNF, methanol production is observed with laser irradiation of 488 nm. The proposed mechanism of $NADP^+$ reduction in this system is described as shown in Fig. 16.[136]

From the proposed mechanism as shown in Fig. 16, $NADP^+$ reduction to NADPH proceeds with the redox coupling Den-NH_2/ Den-NH_3^+ and then CO_2 reduction to methanol with FDH, FldDH and ADH occurs using the redox coupling $NADP^+$/NADPH.

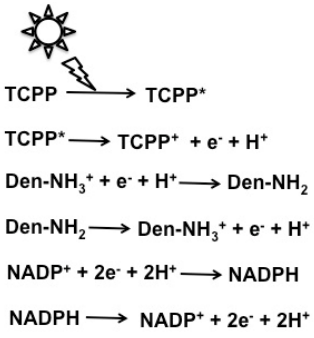

Fig. 16. Proposed mechanism of $NADP^+$ reduction to NADPH in the visible-light driven redox system consisted of an electron donor (D), tetrakis(4-carboxyphenyl)porphyrin (TCCP), Den-NH_2 and $NADP^+$.

The authors of this paper claim that the four-electron oxidation of water into O_2 proceeds with a photosensitization of TCPP, in other word, water molecules works as an electron donor to the oxidized $TCPP^+$. However, O_2 evolution in this system has not been measured yet. As water does not act as an electron donor in the photoredox system with TCPP, in general, NADPH works as an effective electron donor in this system. In this system, since the NADPH is loaded on the Den-TCPP-TOCNF, the substantial photoreduction efficiency of $NADP^+$ to NADPH is not clear. In the future, discussion including photoreduction efficiency of $NADP^+$ to NADPH in addition CO_2 reduction to methanol with Den-TCPP-NADPH (FDH/FldDH/ADH)-TOCNF is necessary.

Photoredox system for light driven CO_2 reduction with biocatalyst via the redox couple of bipyridinium salt

The relationship between the NAD(P)$^+$-depend dehydrogenases and natural co-enzyme NAD(P)$^+$ or NAD(P)H is considered again. For example, the kinetic parameters for the Michaelis constants (K_m) of NAD$^+$ and NADH for FDH from *Candida boidinii* in the formate oxidation to CO_2 and the reverse reaction are determined. The K_m values for NAD$^+$ in the formate oxidation and NADH in the CO_2 reduction to FDH are estimated to be 50 and 2087 mM, respectively. Thus, FDH can be activated by the lower concentration of NAD$^+$, compared with that of NADH (1/400), and the affinity of NAD$^+$ for FDH is higher than that of NADH. Then, what is the K_m values of NAD$^+$ and NADH for other commercially available NAD(P)$^+$-depend dehydrogenases, FldDH, FldDH and ADH? Table 4 shows the summary of previous reported K_m values of NAD$^+$ and NADH for commercially available ADH,[137] AldDH,[138,139] FldDH,[140] and FDH.[141,142]

Table 4. Summary of K_m values of NAD$^+$ and NADH for commercially available FDH, AldDH, FldDH and ADH.

Dehydrogenase	K_m (μM)		Reference
	NAD$^+$	NADH	
FDH	15	9980	141, 142
AldDH	1100	-	138, 139
FldDH	350	-	140
ADH	5.9	122	136

From Table 4, the affinity of NAD$^+$ for all dehydrogenases is overwhelmingly higher than that of NADH. The K_m values of NADH for AldDH from *Yeast* and FldDH from *Pseudomonas sp.* are not reported yet as far as surveyed. No formate reduction to formaldehyde with FldDH from *Pseudomonas sp.* In the presence of NADH is observed. As long as the NAD(P)$^+$/ NADH redox coupling is used, the affinity between NAD(P)H and commercially available NAD(P)$^+$-depend dehydrogenases does not change, therefore, catalytic activities of dehydrogenases cannot be controlled in the visible-light driven redox system using NAD(P)$^+$/ NAD(P)H redox coupling. As the produced NAD(P)H acts as an electron donor and is consumed, moreover, the NAD(P)$^+$/ NAD(P)H redox coupling is not suitable to use for the visible-light driven redox system with the system of a photocatalytic dye and commercially available NAD(P)$^+$-depend dehydrogenases. Moreover, NAD(P)$^+$ is a very expensive biological reagent.

As mentioned above, the redox coupling of NAD(P)$^+$/ NAD(P)H free visible-light driven redox system with commercially available NAD(P)$^+$-depend dehydrogenases is desired. It is necessary to design and to synthesize an electron mediator molecule with simple chemical structure that is easily reduced by visible-light sensitization of a photocatalytic dye and acts as a co-enzyme for commercially available NAD(P)$^+$-depend dehydrogenases. Among the various electron mediators, methylviologen (1,1'-dimethyl-4,4'-bipyridinium salt; MV: chemical structure is shown in Fig. 17) has been widely used as an electron mediator in the visible-light driven redox system with NAD(P)$^+$-depend dehydrogenases for hydrogen production and CO_2 reduction.[143]

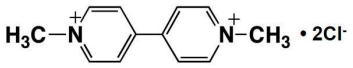

1,1'-Dimethyl - 4,4'- bipyridinium salt (MV)

Fig. 17. Chemical structure of 1,1'-dimethyl-4,4'-bipyridinium salt (MV)

However, there is a serious problem for MV to be used in the visible-light driven redox system using a photocatalytic dye and biocatalyst. Since the single-electron reduced MV is easily oxidized to MV by oxygen, it is used under saturation of inert gas such as nitrogen or argon in the visible-light driven redox system using a photocatalytic dye and biocatalyst for hydrogen production as an example. Since dissolved oxygen in the sample solution can be removed with CO_2 gas, MV can be effectively used as an electron mediator of the visible-light driven CO_2 reduction and utilization system using a photocatalytic dye and biocatalyst. Since 4,4'- or 2,2'-bipyridinium salt (BPs) is easily chemically modified, various BPs are synthesized for the effective electron mediators in the visible-light driven redox system with NAD(P)$^+$-depend dehydrogenases. The chemical structures of various BPs are shown in Fig. 18.[143]

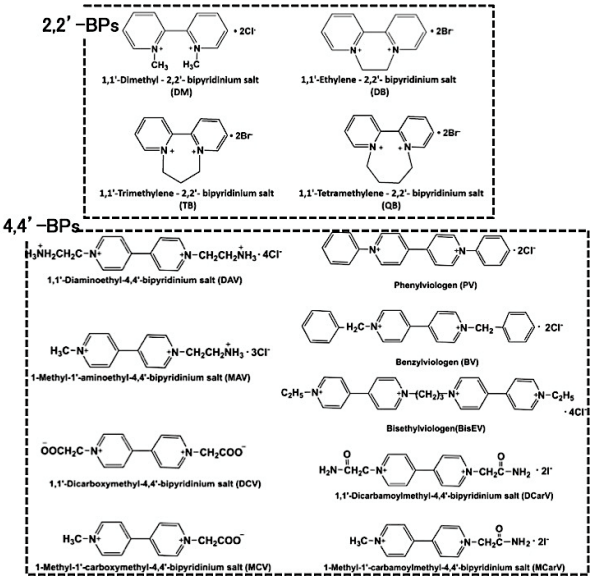

Fig. 18. Chemical structures of various 4,4'- and 2,2'-bipyridinium salts (BPs).

The visible-light driven CO_2 reduction systems with the coupling the reduction of various BPs with $Ru(bpy)_3^{2+}$, water soluble zinc porphyrin or chlorophyll-*a* and commercially available $NAD(P)^+$- depend dehydrogenases have been reported. In this system, the single-electron reduced BPs acts as a co-enzyme for $NAD(P)^+$-depend dehydrogenases instead of NAD(P)H.

The visible-light driven CO_2 reduction to formate consisting of various BPs, $Ru(bpy)_3^{2+}$ as a photocatalytic dye, alkanethiol (RSH) as an electron donor and FDH has been reported as shown in Fig. 19 for the first time. [144-147] The redox processes of 4,4'- and 2,2'-BPs are also shown in Fig. 19.

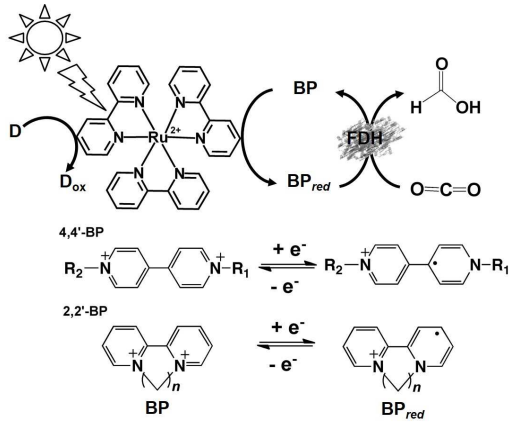

Fig. 19. Scheme of the visible-light driven redox system for CO_2 reduction to formate consisted of an electron donor (D), $Ru(bpy)_3^{2+}$ as a photocatalytic dye, BP and FDH. The redox processes of 4,4'- and 2,2'-BPs are also indicated.

In this report, DM, TB, QB and MV are used as an electron mediator and the single-electron reduced BPs act as the co-enzyme for FDH. Typical reaction sample consists of RSH (10mM), $Ru(bpy)_3^{2+}$ (30 μM), various BPs (1.0 mM) and FDH (0.89 units) in CO_2-saturated buffer solution. The rate of formate production using DM, TB, QB and MV as the electron mediator are estimated to be 0.21, 0.60, 0.30 and 0.75 mM h^{-1}, respectively. By using TB or MV as an electron mediator, effective visible-light driven CO_2 reduction to formate system with FDH is developed.

Furthermore, the effects of the chemical structure and redox potentials of various 2,2'-BPs on the visible-light driven CO_2 reduction to formate with $Ru(bpy)_3^{2+}$ and FDH have been reported.[148] Typical reaction sample consists of triethanolamine TEOA (0.5 M), $Ru(bpy)_3^{2+}$ (0.5 mM), various 2,2'-BPs (3.0 mM) and FDH (8 mg) in CO_2-saturated buffer solution. The concentrations of formate production after 7 h irradiation using DB, TB, QB and MV as the electron mediator are estimated to be 0.50, 0.95, 0.40 and 0.50 mM, respectively. This study showed that compared to systems which used other 2,2'-BPs, the most effective visible-light driven CO_2 reduction to formate with $Ru(bpy)_3^{2+}$ and FDH is achieved by using TB.

Visible-light driven CO_2 reduction to formate using water-soluble zinc porphyrin, zinc tetraphenylporphyrin tetrasulfonate (ZnTPPS) in place of $Ru(bpy)_3^{2+}$ as a photocatalytic dye has also been developed as shown in Fig. 20.[149]

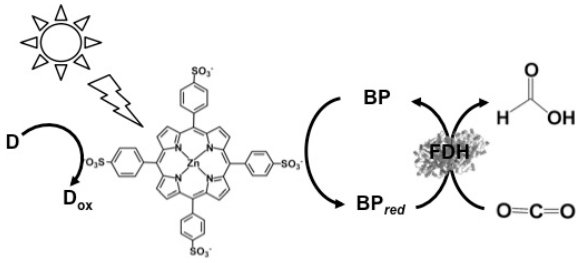

Fig. 20. Scheme of the visible-light driven redox system for CO_2 reduction to formate consisted of an electron donor (D), ZnTPPS as a photocatalytic dye, BP and FDH.

Typical reaction sample consists of TEOA (0.3 M), ZnTPPS (10 μM), 2,2'-BPs (DM, DB, TB, QB and MV) (0.1 mM) and FDH (9.3 μM) in CO_2-saturated buffer solution. The rate of formate production using DM, DB, TB, QB and MV as the electron mediator are estimated to be 18.0, 35.0, 23.5, 13.5 and 22.0 μM h^{-1}, respectively. By using DB as an electron mediator, the effective visible-light driven CO_2 reduction to formate is developed using ZnTPPS.

Table 5 shows the summary of the rate of formate production in the visible-light driven redox system of an electron donor, a photocatalytic dye, 2,2'-BPs and FDH.

Here, the effects of the chemical structure based on the dihedral angles and redox potentials of 2,2'-BPs on the visible-light driven CO_2 reduction to formate with photocatalytic dye and FDH are discussed. The redox potentials ($E_{1/2}$) for DB, TB, QB and DM are estimated to be -0.55, -0.72, -0.82 and -0.89 V (*vs* Ag/AgCl), respectively. The dihedral angles of the single-electron reduced DB, TB, QB and DM calculated by molecular mechanics method are estimated to be about 21, 37, 45, and 55˚, respectively. From these data, 2,2'-BPs with a higher redox potential and small dihedral angle between pyridine-rings are suitable electron mediator for the visible-light driven CO_2 reduction to formate with a photocatalytic dye and FDH.

Table 5. Summary of the rate of formate production in the visible-light driven redox system of an electron donor, a photocatalytic dye, 2,2'-BPs and FDH.

Photocatalytic dye	Electron donor	2,2'-BPs	Rate of formate production (μM h^{-1})	Reference
$Ru(bpy)_3^{2+}$	RSH	DM	210	144
		TB	600	144
		QB	300	144
$Ru(bpy)_3^{2+}$	TEOA	DB	71.4	148
		TB	135.7	148
		QB	57.1	149
ZnTPPS	TEOA	DB	35.0	149
		TB	23.5	149
		QB	13.5	149
		DM	18.0	149

In the visible-light driven CO_2 reduction to formate with photocatalytic dye, 2,2'-BPs and FDH, the single-electron reduced 2,2'- BPs act as a co-enzyme for FDH instead of NAD(P)H. As mentioned above, the total yield of CO_2 reduction to formate in the system consisting of an electron donor, a photocatalytic dye, 2,2'-BPs, and FDH depends on the relative magnitude of the redox potentials of the 2,2'-BPs. As the reduction efficiency of each 2,2'-BPs using the visible-light sensitization of a photocatalytic dye is not the same, thus, the direct interaction between the single-electron reduced 2,2'-BPs and FDH is unclear. The kinetic parameters of the single-electron reduced 2,2'- BPs for the CO_2 reduction to formate with FDH by using an enzymatic kinetic analysis are reported for the first time.[150,151] For an enzymatic kinetic analysis, sodium dithionate is used to chemically prepare the single-electron reduced 2,2'- BPs. It is confirmed that no CO_2 reduction proceeds with only sodium dithionate (in the absence of FDH or 2,2'- BPs). In the viewpoint of affinity of the single-electron reduced 2,2'-BPs for FDH, K_m values of the single-electron reduced DB, TB, QB and DM in CO_2 reduction to formate with FDH are estimated to be 78.4, 142, 165 and 220 μM, respectively. The K_m values of single-electron reduced 2,2'-BPs for FDH also depend on the dihedral angle of pyridine rings of reduced form 2,2'-BPs. As the dihedral angle of pyridine rings in the reduced 2,2'-BPs became smaller, the K_m values became smaller. The single-electron reduced 2,2'-BP with lower K_m value, DB or TB tends to interact with FDH at lower concentration, compared with those of QB and DM. The K_m values for FDH, the dihedral angle and redox potential of reduced form 2,2'-BPs are listed in Table 6.

Comparing the K_m value and the formate production rate in the visible-light driven CO_2 reduction with a photocatalytic dye and FDH, efficient CO_2 reduction is achieved by using a 2,2'-BPs with lower K_m value. As the single-electron reduced DB with small dihedral angle is easy to interact with the binding site of FDH due to small steric hindrance, especially, the effective CO_2 reduction with FDH is accomplished using the other single-electron reduced 2,2'-BPs.

Table 6. Summary of K_m values for FDH, the dihedral angle and redox potential of reduced form 2,2'-BPs.

2,2'-BPs	K_m (μM)	Dihedral angle (°)	Redox potential (V)	Reference
DB	78.4	21	-0.55	150, 151
TB	142	37	-0.72	151
QB	165	45	-0.82	151
DM	220	55	-0.89	150, 151

Various 4,4'-BPs are widely used as electron mediator as well as 2,2'-BPs in the visible-light driven CO_2 reduction to formate with a photocatalytic dye and FDH. As mentioned above, visible-light driven CO_2 reduction to formate with a $Ru(bpy)_3^{2+}$ and FDH using MV as an electron mediator has been reported in the 1980's. After that, visible-light driven CO_2 reduction to formate with a $Ru(bpy)_3^{2+}$ and FDH using various 4,4'-BPs (PV, BV and BisEV) as an electron mediator has been reported. Typical reaction sample consists of triethanolamine TEOA (0.5 M), $Ru(bpy)_3^{2+}$ (0.5 mM), various 4,4'-BPs (3.0 mM) and FDH (8 mg) in CO_2-saturated buffer solution. The concentrations of formate production after 7 h irradiation using PV, BV, and BisEV as the electron mediator are estimated to be 0.20, 0.40 and 0.40 mM, respectively.

For the first example using water-soluble zinc porphyrin as a photocatalytic dye as well as $Ru(bpy)_3^{2+}$, the visible-light driven CO_2 reduction to formate consisting of zinc tetrakis(4-methylpyridiyl)porphyrin (ZnTMPyP) MV, TEOA and FDH also has been reported as shown in Fig. 21. [152-154]

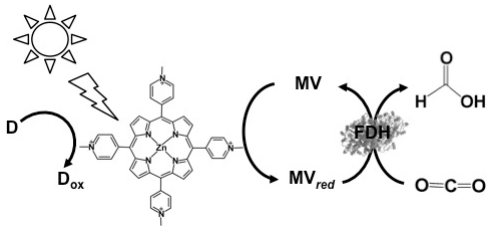

Fig. 21. Scheme of the visible-light driven redox system for CO_2 reduction to formate consisted of an electron donor (D), ZnTMPyP, MV and FDH.

Typical reaction sample is consisted of TEOA (0.3 M), ZnTMPyP (9.0 μM), MV (15 mM), and FDH in CO_2 saturated buffer solution. To develop the effective CO_2 reduction to formate, units of FDH in a solution are varied between 2.5 and 30 units in the report. Formate production increases with FDH activity up to 20 units and then decreases. The concentration of formate production under the optimum condition is estimated to be 60 μM after 3 h irradiation. The turnover number of MV in this system is estimated to be 0.03 min^{-1}. ZnTMPyP is an excellent photocatalytic dye, but its stability is poor for continuous visible-light irradiation. As mentioned above, in contrast, ZnTPPS is an excellent photocatalytic dye with photostability and is widely used in the visible-light driven redox system as shown in Fig. 21. The visible-light driven CO_2 reduction to formate with ZnTPPS and FDH using various 4,4'-BPs as the electron mediators (Fig. 19).

Effect of the ionic-group of 4,4'-BPs as the electron mediator on the visible-light driven CO_2 reduction to formate with the system consisting of ZnTPPS and FDH in the presence of TEOA has been studied.[152, 153] 1,1'-Diaminoethyl- (DAV), 1-aminoethyl-1'-methyl- (AMV), 1-carboxymethyl-1'-methyl- (CMV) and 1,1'-dicarboxymethyl-4,4'-bipyridinium salt (DCV) are synthesized as the 4,4'-BPs with the ionic-group. Typical reaction sample consists of TEOA (0.3 M), ZnTPPS (10 μM), 4,4'-BPs (DAV, AMV, CMV and DCV) (0.1 mM) and FDH (9.3 μM) in CO_2-saturated buffer solution. The rate of formate production using DAV, AMV, CMV and DCV as the electron mediator are estimated to be 120, 100, 50.0 and 40.0 μM h^{-1}, respectively. By using 4,4'-BPs with cationic amino-group, DAV or AMV as an electron mediator, the effective visible-light driven CO_2 reduction to formate is observed compared with the 4,4'-BPs with anionic carboxy-group, CMV or DCV. The formate production rate with DAV is about 3.2 times larger than that of the system with DCV. The single-electron reduced DAV and MAV are used as the effective electron mediator for FDH in the visible-light driven CO_2 reduction to formate.

As the carbamoyl-group of NAD^+ is captured at the active site of FDH via the hydrogen bond, thus, the single-electron reduced 4,4'-BPs with carbamoyl-group can be an effective co-enzyme of FDH in the CO_2 reduction to formate.[157] 1,1'-Dicarbamoylmethyl-4,4'-bipyridinium salt (DCarV) and 1-carbamoylmethyl-1'-methyl-4,4'-bipyridinium salt (MCarV) as the 4,4'-BPs with carbamoyl-group are synthesized to improve the affinity for FDH. Typical reaction sample consists of TEOA (0.3 M), ZnTPPS (10 μM), 4,4'-BPs with carbamoyl-group (DCarV and MCarV) (0.1 mM) and FDH (9.3 μM) in CO_2-saturated buffer solution. The rate of formate production using DCarV and MCarV as the electron mediator are estimated to be 95.0 and 120 μM h^{-1}, respectively. By using MCarV, especially, the efficiency of visible-light driven CO_2 reduction to formate with the system consisting of ZnTPPS and FDH in the presence of TEOA is improved about 60 % than that using MV. From these results, carbamoyl-group in 4,4'-BP affected the electron transfer, leading the improvement of CO_2 reduction to formic acid with FDH.

Table 7 shows the summary of the rate of formate production in the visible-light driven redox system of an electron donor, a photocatalytic dye, 4,4'-BPs and FDH.

The direct interaction between the single-electron reduced 4,4'-BPs and FDH also is unclear. The kinetic parameters of the single-electron reduced 4,4'-BPs for the CO_2 reduction to formate with FDH by using an enzymatic kinetic analysis also are reported for the first time.[158,159] In the viewpoint of affinity of the single-electron reduced 4,4'-BPs for FDH, K_m values of the single-electron reduced DAV, MAV, MV, MCV and DCV in CO_2 reduction to formate with FDH are estimated to be 17.0, 118, 212, 292 and 370 μM, respectively. The K_m values of single-electron reduced 4,4'-BPs for FDH also depend on the number of positive charge of reduced form 4,4'-BPs. The numbers of electron charges in the single-electron reduced 4,4'-BPs are DAV (+3), MAV (+2), MV (+1), MCV (0) and DCV (-1), respectively.

Table 7. Summary of the rate of formate production in the visible-light driven redox system of an electron donor, a photocatalytic dye, 4,4'-BPs and FDH.

Photocatalytic dye	Electron donor	4,4'-BPs	Rate of formate production (μM h^{-1})	Reference
$Ru(bpy)_3^{2+}$	TEOA	MV	71.4	148
		PV	28.6	148
		BV	57.1	148
		BisEV	57.1	148
ZnTMPyP	TEOA	MV	20.0	152-154
ZnTPPS	TEOA	MV	60.5	155, 156
		DAV	120	155, 156
		MAV	100	156
		MCV	50.0	156
		DCV	40.0	156
		DCarV	95.0	157
		MCarV	120	157

The formate production is proportional to the numbers of electron charges in the single-electron reduced 4,4'-BPs. This results indicate that the formate production in the reaction depends on ionic-substituted groups in the single-electron reduced 4,4'-BPs. The K_m values for FDH, numbers of electron charges of reduced form 4,4'-BPs are listed in Table 8.

Comparing the K_m value and the formate production rate in the visible-light driven CO_2 reduction with ZnTPPS and FDH, efficient CO_2 reduction is achieved by using a DAV or MAV with lower K_m value.

Table 8. Summary of K_m values for FDH, the numbers of electron charges of reduced form 4,4'-BPs.

4,4'-BPs	K_m (μM)	Numbers of electron charges of reduced form 4,4'-BPs	Reference
DAV	17.0	3	158
MAV	118	2	158, 159
MV	212	1	158, 159
MCV	292	0	159
DCV	370	-1	159

More notably, the oxidized BPs do not act as a co-enzyme for FDH in the formate oxidation to CO_2. That is, only single-electron reduced BPs act as the co-enzyme for FDH in the CO_2 reduction to formate. This property of BPs is not found in natural co-enzymes, NAD^+ and NADH.

As described above, by using various BPs, thus, CO_2 reduction to formate rate can be controlled without changing the structure of FDH.

In addition, visible-light driven CO_2 reduction to formate with the system consisting of chlorophyll-*a* (MgChl-*a*) as a photocatalytic dye, MV and FDH in the presence of electron donor as shown in the Fig. 22 is also accomplished.[160]

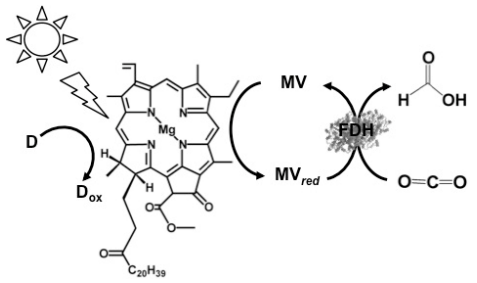

Fig. 22. Scheme of the visible-light driven redox system for CO_2 reduction to formate consisted of an electron donor (D), chlorophyll-*a* (MgChl-*a*), MV and FDH.

As the visible-light driven redox system for CO_2 reduction to formate is consisted of an electron donor (D), a photocatalytic dye, BP and FDH is accomplished, methanol production is developed by adding AldDH and ADH in this system as shown in Fig. 23. By using this system, ZnTPPS or metal-free TPPS (H_2TPPS) is used as a photocatalytic dye. Visible-light driven CO_2 reduction to methanol with the system of TEOA, ZnTPPS, MV, FDH, AldDH, and ADH has been reported for the first time.[161-163]

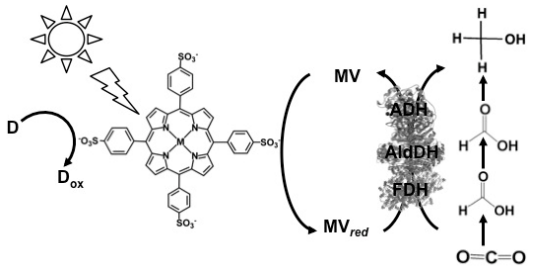

Fig. 23. Scheme of the visible-light driven redox system for CO_2 reduction to methanol consisted of an electron donor (D), MTPPS (M: Zn or H_2), MV, FDH, AldDH and ADH.

Typical sample solution is consisted of TEOA (0.3 M), ZnTPPS (0.1 μM), MV (0.1 mM), FDH (12.5 units), AldDH (12.5 units), ADH (12.5 units) and sodium bicarbonate ($NaHCO_3$) instead of CO_2 in the buffer solution. When a sample solution containing ZnTPPS, MV, TEOA, FDH, AldDH, ADH and $NaHCO_3$ is irradiated, the concentration of methanol production is detected to be 4.5 μM after 3 h irradiation. The conversion yield of HCO_3^- to methanol is estimated to be 4.5 % after 3 h irradiation (initial concentration of HCO_3^- 100 μM). In this system, the single-electron reduced MV acts as a shared co-enzyme for three dehydrogenases FDH, AldDH and ADH.

However, the yield for CO_2 reduction to methanol with this system is low. To improve the efficiency of CO_2 reduction to methanol with this system, it is necessary to clarify the interaction between FDH, AldDH or ADH and the single-electron reduced MV. The kinetic parameters for formaldehyde reduction to methanol with ADH and the single-electron reduced MV are determined by using enzymatic kinetic analysis. The K_m value of the single-electron reduced MV for ADH in the reduction of formaldehyde to methanol is estimated to be 312 μM. The K_m value of the single-electron reduced MV for ADH is almost the same values for FDH indicating that the affinity of the single-electron reduced MV for ADH is equal to that for FDH.[163]

On the basis of this result, the improvement for the CO_2 reduction to methanol under visible-light irradiation is attempted with the system consisting of TEOA, H_2TPPS, MV, FDH, AldDH and ADH. Three dehydrogenases are adjusted to the same concentration (not same units). When the sample solution consisting of H_2TPPS (100 μM), MV (2.0 mM), TEOA (0.3 M), FDH (2.0 μM), AldDH (2.0 μM) and ADH (2.0 μM) in CO_2 saturated 50 mM sodium pyrophosphate buffer is irradiated, the methanol is produced with increasing irradiation time and methanol concentration produced is estimated to be 6.8 μM after 100 min irradiation. Further improvement in the visible-light driven CO_2 reduction to methanol efficiency is desired in the system of TEOA, H_2TPPS, MV, FDH, AldDH and ADH.

In addition, the light driven CO_2 reduction to methanol using methanol dehydrogenase (MDH) from *Bacillus* (EC 1.1.1.244), ZnS as a photocatalytic dye and pyrroloquinoline quinone (PQQ) [164] as an electron mediator has also been reported as shown in Fig. 24. The redox process of PQQ [165-169] also is indicated in Fig. 24.

In this system, 2-propanol is used as an electron donor. Typical sample solution is consisted of the CO_2-saturated ZnS microcrystalline colloid containing PQQ (5 mM) and MDH (2 units). When a sample containing ZnS, PQQ and MDH in CO_2 saturated condition is irradiated with UV-light, formate and methanol productions are observed. A saturation tendency of the methanol production appears when the amount of methanol is accumulated to *ca.* 0.25 mM after 1 h irradiation. On the other hand, the concentration of formate is increased with increasing irradiation time. After 3 h irradiation, 0.50 mM of formate is produced with this system.

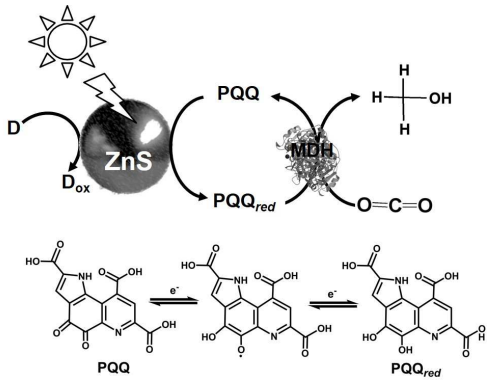

Fig. 24. Scheme of the light driven redox system for CO_2 reduction to methanol consisted of an electron donor (D), ZnS, PQQ and MDH.

The proposed mechanism of light driven CO_2 reduction to methanol with the system of an electron donor, ZnS, PQQ and MDH is shown in Fig. 25. In this system, there are two photoredox processes; 1) CO_2 reduction to formate with the photocatalytic reaction of ZnS and 2) formate reduction to methanol with ZnS via the PQQ /PQQ_{red} redox coupling. Thus, rate of CO_2 reduction to formate with the photocatalytic reaction of ZnS is larger than that of formate reduction to methanol.

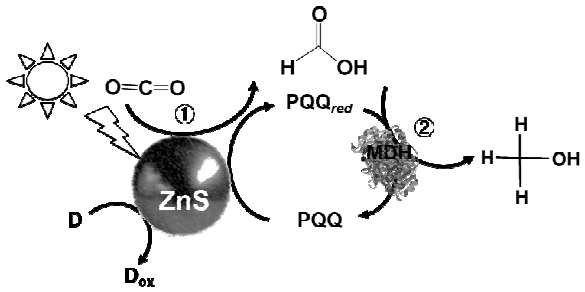

Fig. 25. Proposed mechanism for light driven CO_2 reduction to methanol consisted of an electron donor (D), ZnS, PQQ and MDH.

Next, light driven CO_2 reduction to CO with the systems of a photocatalytic dye and carbon monoxide dehydrogenase (CODH) from *Carboxydothermus hydrogenoformans* (EC1.2.7.4) are introduced. By using CODH in the light driven

CO_2 reduction to CO with a photocatalytic dye, an electron mediator such as MV is unnecessary.

Typical light driven CO_2 reduction to CO with the systems of a photocatalytic dye and CODH are shown in Fig. 26.[170-173]

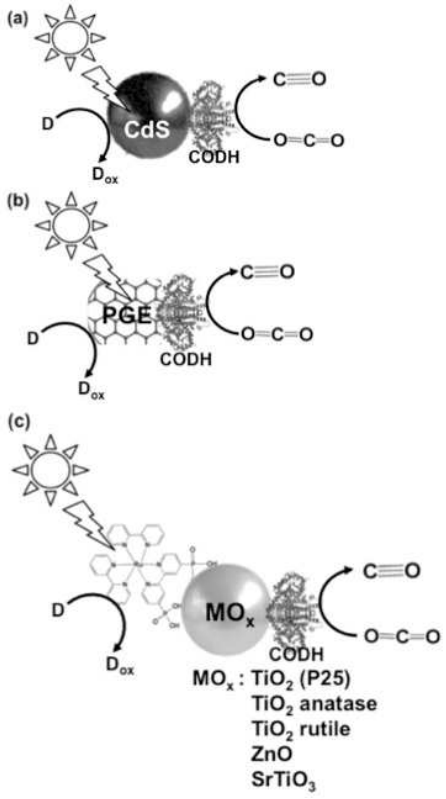

Fig. 26. Scheme of the light driven redox system for CO_2 reduction to CO consisted of an electron donor (D), a photocatalytic dye (a: CdS, b: Pyrolytic graphite "edge" (PGE), c: dye-modified metal oxide) and CODH.

Light driven CO_2 reduction to CO with the systems of a photocatalytic dye and CODH are classified into three categories based on the photocatalytic dye; a) CdS,[172] b) pyrolytic graphite "edge" (PGE) [173] and c) dye-modified metal oxide (TiO_2, ZnO or $SrTiO_3$). [170, 171]

The effect of an electron donor on the light driven CO_2 reduction to CO with the system of CdS and CODH is investigated. Typical reaction sample is consisted of CODH immobilized CdS based quantum dots (CODH-QDs) and various electron donor (ascorbate, EDTA or TEOA: 0.2 M, or KI :0.3 M) in CO_2 saturated 0.35 M 2-(*N* -morpholino)ethanesulfonic acid buffer. By using EDTA as an electron donor, 3.0 µmol of CO is evolved in the light driven redox system with CODH-QDs after 5 h irradiation. By using TEOA, in contrast, 0.5 µmol of CO is evolved in the system with CODH-QDs after 5 h irradiation. Moreover, no CO evolution is observed in the system with CODH-QDs by using ascorbate or KI.

By using CODH and $[Ru(bpy)_2(4,4'\text{-}(PO_3H_2)_2\text{-}bpy)]Br_2$ (RuP) modified TiO_2 (P25) as a photocatalytic dye (RuP-TiO_2-CODH), at pH 6 and 20 °C, the visible-light driven CO_2 reduction to CO proceeds and 5 µmol of CO is produced after 4 h irradiation. At the reaction temperature of 50 °C, 12 µmol of CO is produced in this system after 4 h irradiation. By using CODH and $[Ru(bpy)_2(4,4'\text{-}(PO_3H_2)_2\text{-}bpy)]Br_2$ (RuP) modified TiO_2 (anatase), TiO_2 (rutile), ZnO and $SrTiO_3$, 4.3, 0, 0.55 and 0.5 µmol of CO, respectively are produced after 4 h irradiation.

By using CODH immobilized PGE as a photocatalytic dye, only photoelectrochemical properties of CO_2 reduction to CO are investigated.[173]

Photoredox system for light driven CO_2 utilization

Photoredox system for light driven CO_2 utilization with biocatalyst via the redox couple of $NAD(P)^+$/ NAD(P)H

As mentioned previous section, the light driven redox systems for the CO_2 reduction with $NAD(P)^+$-dependent dehydrogenase have been introduced. As the system is only CO_2 reduction based on the multi-electrons-protons coupling reaction with visible light energy, thus, the number of carbon in product dose not extended.

In this section, let us focus on light driven redox systems with biocatalyst for building carbon-carbon bonds from CO_2 as the carbon feedstock. As mentioned above, ME and IDH are attractive biocatalysts for this target, and CO_2 is bonded to the organic molecule as a carboxy-group. [174]

A visible-light driven redox system with ME that exploit reduction of $NADP^+$ to NADPH as the electron mediator has been described for the first time. In this case, the use of $Ru(bpy)_3^{2+}$, MV, FNR and 2-mercaptoethanol led to malate production from HCO_3^- and pyruvate, as shown in Fig. 27.[145, 175]

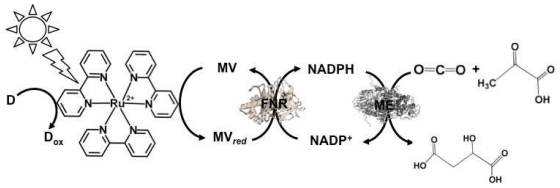

Fig. 27. Scheme of the visible-light driven redox system for malate production from pyruvate and CO_2 consisted of $Ru(bpy)_3^{2+}$, MV, FNR, $NADP^+$, ME and 2-mercaptoethanol.

In this system, the single-electron reduced MV dose not act as co-enzyme for ME in the reaction of malate production from CO_2 and pyruvate. Thus, the redox system of $NADP^+$/NADPH with FNR is needed to integrate into the system. FNR catalyzes the reduction of $NADP^+$ to NADPH coupling redox of ferredoxin as shown in Fig. 12. Moreover, FNR also catalyzes the reduction of $NADP^+$ to NADPH coupling redox of MV and the single-electron reduced MV (MV_{red}) as shown in Fig. 28.[180]

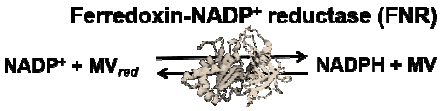

Fig. 28. Reaction scheme of FNR for $NADP^+$ reduction to NADPH in the presence of the single-electron reduced MV (MV_{red}).

The system is composed of a Tris buffer (4.2 ml; 0.2 M; pH 8.0) including pyruvic acid (470 mM), MV (0.19 mM), $NADP^+$ (0.18 mM), $Ru(bpy)_3^{2+}$ (21 μM), $MgCl_2$, (9.5 μM), $NaHCO_3$ (0.2 M) and 2-mercaptoethanol (19 mM). To this solution are added FNR (0.2 units) and ME (1.33 units). After 2 h irradiation to this system, 3.0 mM of malate is produced and yield for malate production from HCO_3^- and pyruvate has been estimated to be 3.6 % after 2 h irradiation.

IDH biocatalyst coupled with a visible-light driven redox system consisting in $NADP^+$ with a system containing $Ru(bpy)_3^{2+}$, MV, FNR and DL-dithiothreitol (DTT) as an electron donor for isocitrate production from HCO_3^- and α-oxoglutarate as shown in Fig. 29 also has been reported. [145,180]

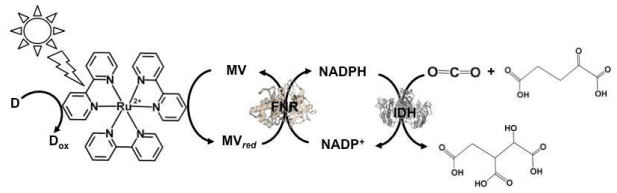

Fig. 29. Scheme of the visible-light driven redox system for isocitrate production from α-oxoglutarate and CO_2 consisted of $Ru(bpy)_3^{2+}$, MV, FNR, $NADP^+$, IDH and DTT.

The system is composed of a Tris buffer (4.2 ml; 0.2 M; pH 7.2) including $Ru(bpy)_3^{2+}$ (14 μM), MV (0.17 mM), $NADP^+$ (0.17 mM), $MnCl_2$, (1.7 mM), $NaHCO_3$ (0.17 M), α-oxoglutaric acid (42 mM) and DTT (8.3 mM). The following biocatalysts are added FNR (0.2 units) and IDH (0.47 units) immobilized on poly(acrylamide-*co*-*N*-acryloxysuccinimide). After 2 h irradiation to this system, 0.6 mM of isocitrate is produced and yield for isocitrate production from HCO_3^- and α-oxoglutarate is estimated to be 1.9 % after 2h irradiation.

A different approach involving with ME and reduction of $NADP^+$ with a system containing TiO_2 semiconductor or CdS photocatalyst, MV, FNR and lactate or 2-mercaptoethanol an electron donor for the malate production from CO_2 and pyruvate acid as shown in Fig.30 .[181]

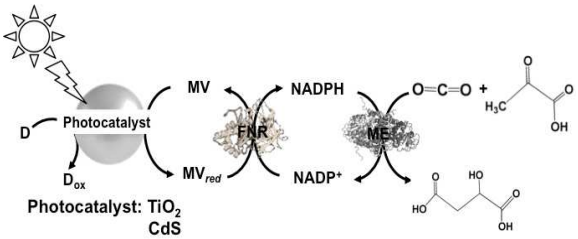

Fig. 30. Scheme of the light driven redox system for malate production from pyruvate and CO_2 consisted of a photocatalyst (TiO_2 or CdS), MV, FNR, $NADP^+$, ME and lactate or 2-mercaptoethanol.

By using TiO_2 as a photocatalyst, the solution is 10 mL of CO_2-saturated Tris buffer containing MV (1.0 mM), $NADP^+$ (0.1 mM), FNR (0.2 unit), ME (1.0 unit), pyruvic acid (2.0 mM), 2-mercaptoethanol (27 mM) and TiO_2. When the solution is irradiated with UV-light, 0.3 mM of malate is produced after 5 h irradiation. By using CdS as a photocatalyst, in contrast, 1.0 mM of malate is produced after 5 h irradiation under the same condition using TiO_2. It is thought that at these optimum conditions, *ca.* 50% of pyruvate is converted to malate at CdS and *ca.* 15 % at TiO_2 semiconductor, respectively.

As lactate oxidation to pyruvate with the photocatalytic function of CdS proceeds, moreover, light driven malate production from CO_2 and lactate via the pyruvate with the system of CdS and ME is developed. The sample solution is ME (5.0 units) in 10 cm^3 of 10 mL of CO_2-saturated Tris buffer containing MV (1.0 mM), $NADP^+$ (0.1 mM), FNR (0.2 unit), $NADP^+$ (0.1 mM), sodium lactate (100 mM) and CdS (1.25 mM). After 6 h irradiation, concentrations of malate and pyruvate are determined to be 0.2 and 0.7 mM, respectively. In this system, it is achieved to the malate production from CO_2 and pyruvate as an intermediate produced from lactate (electron donor) oxidation with CdS.

A visible-light driven catalytic system consisting of NADH as the electron donor, ZnChl-e_6 (Chlorin-e_6, formed by the hydrolysis of chlorophyll-*a*), MV, FNR, $NADP^+$ and ME has been reported as shown in Fig. 31.[182, 183]

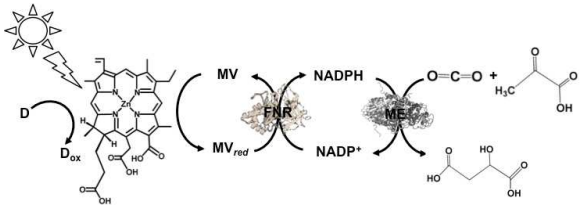

Fig. 31. Scheme of the visible-light driven redox system for malate production from pyruvate and CO_2 consisted of ZnChl-e_6, MV, FNR, $NADP^+$, ME and NADH.

A sample solution is composed of NADH (30 mM), Zn Chl-e_6 (50μM), MV (1.0 mM), FNR (4.0 units), $NADP^+$ (10 mM), pyruvic acid (10 mM), $NaHCO_3$(10 mM) and ME (4.5 units) in Bis-Tris buffer (pH 8.0) . After 3 h irradiation for this system, the concentration of malate production is 0.65 mM and the ratio of pyruvate to malate is estimated to be about 6.5 %.

These results show that the malate production proceeds by combination of the $NADP^+$ reduction to NADPH using the photocatalytic dye with FNR via the redox coupling MV/MV_{red} and biocatalytic conversion of pyruvate and CO_2 to malate. To simplify this system, $NADP^+$ reduction to NADPH with the system of chemically-modified Chl-*a* and FNR without the redox coupling MV/MV_{red} is attempted.

The visible-light driven redox system with ME and reduction of $NADP^+$ with a system containing ascorbate as an electron donor, the polyethylene glycol modified chlorophyll-*a* (PEG-Chl-*a*) and FNR as shown in Fig. 32 has been exploited for the production of malate from CO_2 and pyruvate.[184] As $NADP^+$ directly is reduced to NADPH with FNR and PEG-Chl-*a* in this reaction, it is not necessary to add the MV as an electron mediator.

A sample solution is composed of the PEG-chlorophyllin conjugate (15 μM), ascorbate (6.0 mM), $NaHCO_3$ (180 mM), $MgCl_2$ (15 mM), pyruvate (0.8 mM), $NADP^+$ (3.2 mM), FNR (2.5 units) and ME (5.0 units) in 10 mL of 50 mM phosphate buffer at pH 7.4. The concentration of malate produced is estimated to be 75 μM after 3 h visible light irradiation.

The yield of malate from pyruvate and HCO_3^- is estimated to be 0.041 %.

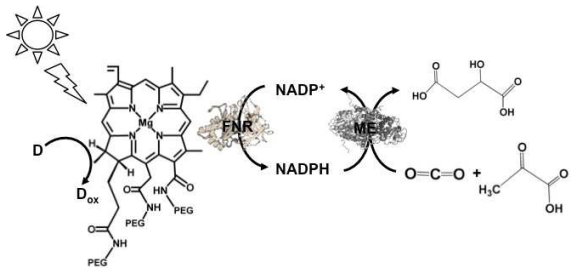

Fig. 32. Scheme of the visible-light driven redox system for malate production from pyruvate and CO_2 consisted of PEG-Chl-*a*, FNR, $NADP^+$, ME and ascorbate

Photoredox system for light driven CO_2 utilization with biocatalyst via the redox couple of bipyridinium salt

The light driven redox system for building carbon-carbon bond from CO_2 and organic molecule with a photocatalytic dye and biocatalyst using redox coupling $NADP^+$/NADPH is very complicated, however, it is necessary to simplify by an electron mediator instead of $NADP^+$ reduction part with FNR as shown in Fig. 33.

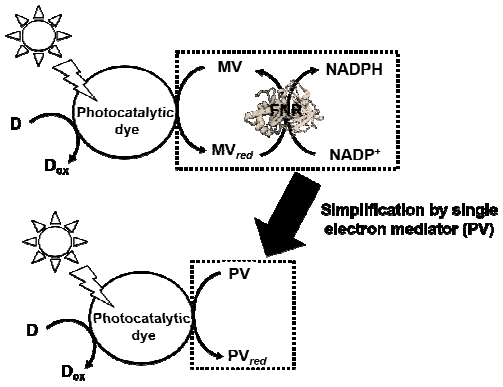

Fig. 33. Scheme of the light driven redox system for $NADP^+$ reduction to NADPH with the system of an electron donor, a photocatalytic dye, MV, FNR (upper) and simplified system using single electron mediator reduction (lower).

To develop the simplified visible-light driven redox system for building carbon-carbon bond from CO_2 and organic molecule using the system of a photocatalytic dye and biocatalyst without redox coupling $NADP^+$/NADPH, the electron mediator that shows the same behavior as a $NADP^+$ or NADPH is necessary. 1,1'-Diphenyl-4,4'-bipyridinium salt (phenylviologen) derivatives (PVs) have received much attention to the electron mediator with same behavior as a $NADP^+$ or NADPH, because PVs have a lower first and second reduction potentials compared with the 2,2'- or 4,4'-BPs.[185] Chemical structures of 1,1'-diphenyl-4,4'-bipyridinium salt derivatives (PVs) are shown in Fig. 34.

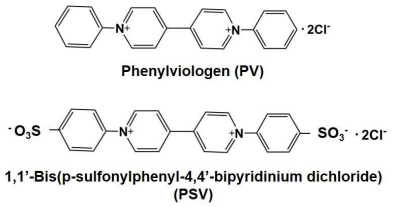

Fig. 34. Chemical structures of 1,1'-diphenyl-4,4'-bipyridinium salt (PV) and 1,1`-bis (*p*-sulfonyphenyl-4,4'-bipyridinium dichloride (PSV).

A visible-light driven redox system with ME that exploit reduction of PV as the electron mediator has been described for the first time. In this case, the use of MTPPS (M: Zn or H_2), PV and TEOA led to malate production from CO_2 and pyruvate, as shown in Fig. 35.[186-188] The redox process of PV also is indicated in Fig. 35.

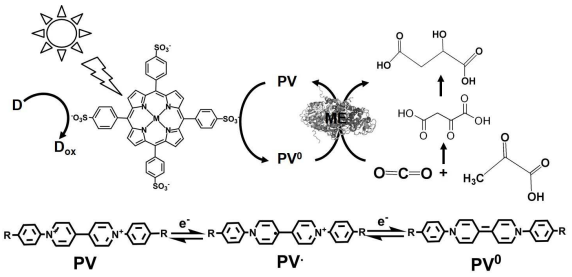

Fig. 35. Scheme of the visible-light driven redox system for malate production from pyruvate and CO_2 consisted of an electron donor, MTPPS, PV and ME. The redox process of PV also is indicated. The single- and double- electron reduced PV are abbreviated as $PV^{\bullet}$ and PV^0, respectively.

The reduction potentials of PSV and PV are summarized in Table 9. The reduction potentials of MV also is listed as a reference in the table. The single (E_{red1}) and double (E_{red2}) electron reduction potentials of PVs are determined by cyclic voltammetry using an Ag/AgCl electrode as a reference electrode.

The single and double electron reduction potentials of PV are estimated to be -0.39 and -0.74 V, respectively. On the other hand, the single and double-electron reduction potentials of PSV are estimated to be -0.38 and -0.72 V, respectively. Compared to the reduction potentials of PV and PSV, there are little difference, so it is considered that the sulfo-group has little effect on the reduction potential. The single and double electron reduction potentials of PVs are lower than the values for MV (−0.67 and −1.05 V, respectively). Thus, the single and double-electron reduced PVs could be easily produced with the photocatalytic dye.

Table 9. Summary of the reduction potentials of PSV, PV and MV.

BPs	Single-electron reduction potential (E_{red1}) (V)	Double-electron reduction potential (E_{red2}) (V)	Reference
PSV	-0.38	-0.72	187, 188
PV	-0.39	-0.74	186
MV	-0.67	-1.05	186-188

By using PV as an electron mediator, the visible-light driven malate production from pyruvate and CO_2 with the system of

TEOA, H_2TPPS, PV and ME is developed. For PV photoreduction, the sample solution is consisted of TEOA (0.3 M), ZnTPPS (10 mM) and PV (0.1 mM) in 5.0 mL of 10 mM bis-tris buffer (pH 7.4). When this sample solution is irradiated, the absorption band due to the double-electron reduced PV is increased with increasing irradiation time. The redox potentials of the exited triplet state of H_2TPPS in buffer aqueous, $E(H_2TPPS^+/\ ^3H_2TPPS^*)$ and $E(^3H_2TPPS^*/H_2TPPS)$ are estimated to be −0.70 and 0.40 V using electrochemical and photochemical measurements, respectively, thus allowing for the production of the single- or double-electron reduced PV.

For the visible-light driven malate production from CO_2 and pyruvate with H_2TPPS, PV and ME in the presence of co-factor $MgCl_2$, a sample solution is composed of TEOA (0.2 M), H_2TPPS (40 μM), PV (0.4 mM), pyruvate (12 mM), MgCl (10 mM). When this sample solution is irradiated, the concentration of malate and oxaloacetate increased with the irradiation time. The concentration of malate production is estimated to be 565 μM after 3 h irradiation. On the other hand, the concentration of oxaloaxetate is estimated to be 1.0 mM after 3 h irradiation. The yield of pyruvate to malate is calculated to be 4.7%.

As both the single and the double-electron reduction state of PV are insoluble in an aqueous solution, however, PV is not suitable for homogenous visible-light driven redox system. Thus, the water-soluble PV derivative, PSV is used as an electron mediator in the visible-light driven redox system.

For PSV photoreduction, the sample solution is consisted of TEOA (0.3 M), ZnTPPS (10 μM) and PSV (0.1 mM) in 5.0 mL of 10 mM bis-tris buffer (pH 7.4). When this sample solution is irradiated, the absorption band due to the double-electron reduced PSV also is increased with increasing irradiation time.

For the visible-light driven malate production from CO_2 and pyruvate with TEOA, H_2TPPS, PV and ME in the presence of co-factor $MgCl_2$, a sample solution is composed of TEOA (0.2 M), H_2TPPS (40 μM), PSV (0.4 mM), pyruvate (12 mM), MgCl (10 mM). When this sample solution is irradiated, the concentration of malate and oxaloacetate increased with the irradiation time. In the system with PSV, as the visible-light irradiation started, the concentration of oxaloacetate increased within 1 h, and then decreased. On the other hand, the concentration of malate increased with decreasing concentration of oxaloacetate. Thus, oxaloacetate is formed as an intermediate and then reduced to malate. The malate concentration after 3 h irradiation is estimated to be 604 μM. The yield of pyruvate to malate is calculated to be 5.0 %.

Table 10 shows the summary of the visible-light driven malate production from CO_2 and pyruvate with TEOA, H_2TPPS, PVs and ME.

Table 10. Summary of the visible-light driven malate production from CO_2 and pyruvate with TEOA, H_2TPPS, PVs and ME.

PVs	Malate production after 1 h irradiation (μM)	Yield of pyruvate to malate	Reference
PV	565	4.7	186
PSV	604	5.0	187, 188
MV	0	0	186-188

From these results, PVs^0 is used for building C-C bonds from CO_2 and pyruvate to produce oxaloacetate and $PSV^\bullet$ is used for the reduction of carbonyl-group of oxaloacetate to malate, respectively. The possible mechanism in the visible-light driven redox system for malate production based on the building C-C bonds from CO_2 and pyruvate is shown in Fig. 36.

At first, the hydrogen in pyruvate is abstracted by PV^0 and then CO_2 is bonded to pyruvate derivative as a carboxy-group based on the building C-C bonds from CO_2, resulting the oxaloacetate production. Finally, the oxaloacetate is reduced to malate by $PV^\bullet$.

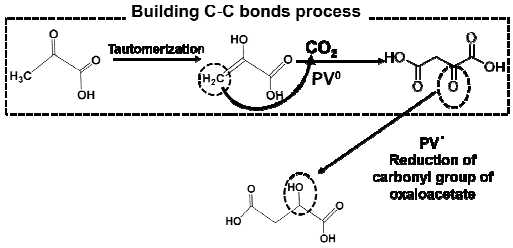

Fig. 36. The possible mechanism for malate production based on the building C-C bonds from CO_2 and pyruvate using PV as an electron mediator in the visible-light driven redox system.

Therefore, the visible light-driven oxaloacetate and malate productions based on ME-catalyzed building carbon-carbon bonds from pyruvate and CO_2, using the photoreduction of PV as an electron mediator with water-soluble porphyrin in the presence of TEOA, is developed for the first time.

The detailed mechanisms underlying oxaloacetate production from CO_2 and pyruvate based on the carbon-carbon bonds using the double-electron reduced PV produced in the photoredox system.

The light driven isocitrate production from CO_2 and α-oxoglutarate with a phtocatalytic dye, CdS and IDH using MV redox coupling without FNR as shown in Fig. 37 has been reported.[189]

The sample solution is composed of 0.2 M Tris buffer containing TEOA (2.0 M), MV (1.0 mM), IDH (0.8 unit), CdS (0.016 mol), α-oxoglutaric acid (10 mM). The isocitrate production proceeds linearly with the irradiation time for 8 h and then beyond that the production decreases gradually, resulting in the complete suppression after 20 h. The amount of isocitrate is estimated to be 8.0 μmol after 20 h.

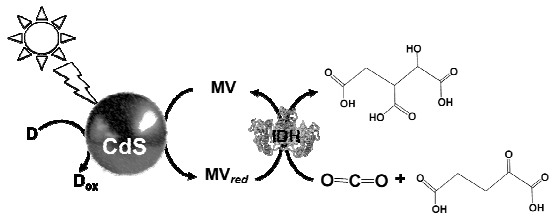

Fig. 37. Scheme of the light driven redox system for isocitrate production from CO_2 and α-oxoglutarate with a phtocatalytic dye, CdS and IDH with MV redox coupling.

Other photoredox system for light driven molecular conversion

The visible-light driven redox systems of the photocatalytic dye and biocatalyst are developed not only for CO_2 reduction and utilization but also for molecular conversion. In this section, some studies on the visible-light driven redox system for molecular conversion with a photocatalytic dye and a biocatalyst are introduced.

The visible-light driven acetate reduction to ethanol with an electron donor (in this system NADPH), ZnChl-e_6, MV, AldDH and ADH as shown in Fig. 38 is developed.[190] In this system, acetate reduction to ethanol via acetaldehyde with AldDH and ADH using the single-electron reduced MV by visible-light sensitization of ZnChl-e_6.

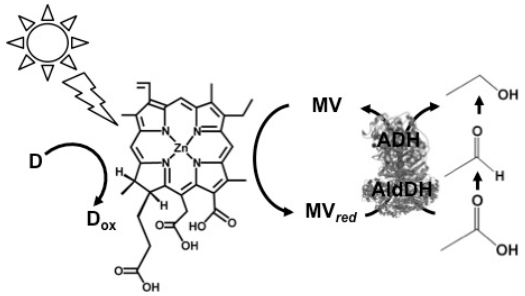

Fig. 38. Scheme of the visible-light driven redox system for acetate reduction to ethanol with an electron donor, ZnChl-e_6, MV, AldDH and ADH.

The sample solution is consisted of ZnChl-e_6 (100 μM), MV (12 mM), NADPH (3.3 mM), AldDH (0.22 μM), ADH (6.7 nM) and sodium acetate (30 mM) in 50 mM sodium pyrophosphate buffer (pH 7.4). When this sample solution is irradiated, 1.4 mM of ethanol is produced after 150 min irradiation. In this system, the single-electron reduced MV acts as a co-enzyme for AldDH and ADH in the acetate and acetaldehyde reduction.

Lactate based polymers (PLAs) are introduced by Watson, and have been received much attention as biodegradable polymers as environmentally friendly materials.[191] To develop the functional PLAs, highly optical purified lactate is desirable. Biocatalytic pyruvate reduction to lactate with commercially available lactate dehydrogenase (LDH) from *Pig heart* (EC 1.1.1.27) as highly optical purity and is suitable for the starting material of PLAs. LDH catalyzes the reaction of lactate oxidation to pyruvate in the presence of NAD^+ and the reversed reaction of pyruvate reduction to lactate in the presence of NADH as shown in Fig. 39.[182,193]

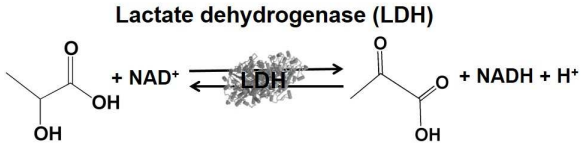

Fig. 39. Reaction schemes of lactate dehydrogenase (LDH).

By using LDH as a biocatalyst, the visible-light driven pyruvate reduction to lactate with an electron donor (in this system TEOA), ZnTMPyP MV and LDH as shown in Fig. 40 is developed.[194]

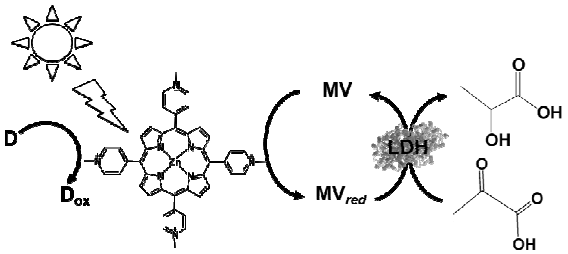

Fig. 40. Scheme of the visible-light driven redox system for pyruvate reduction to lactate with an electron donor (in this system TEOA), ZnTMPyP MV and LDH.

For the visible-light driven lactate production, a sample solution is consisted of TEOA (0.3 M), ZnTMPyP (9.0 μM), MV (60 μM), pyruvic acid (0.1 mM) and LDH (20 units) in 3.0 mL of 10 mM phosphate buffer (pH 7.0). When this sample solution is irradiated, 0.17 mM of lactate is produced after 4 h irradiation. In this system, the single-electron reduced MV acts as a co-enzyme for LDH in the pyruvate reduction to lactate.

Biocatalyst for the visible-light driven ammonia utilization also has been paid attention. Among the biocatalysts for ammonia utilization, $NAD(P)^+$-dependent dehydrogenases can be used for the visible-light driven redox system with a photocatalytic dye. Commercially available glutamate dehydrogenase (GluDH) from *Yeast* (EC 1.4.1.4) catalyzes the reaction of 2-oxoglutarate and NH_4^+ production from *L*-glutamate in the presence of $NADP^+$ and the reversed reaction of *L*-glutamate production from 2-oxoglutarate and NH_4^+ in the presence of NADPH as shown in Fig. 41.[195-197]

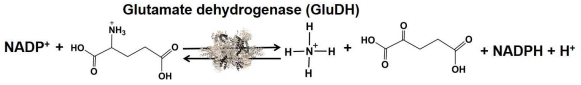

Fig. 41. Reaction schemes of glutamate dehydrogenase (GluDH).

By using GluDH as a catalyst for *L*-glutamate production from 2-oxoglutarate and NH_4^+ in the presence of NADPH, the building nitrogen-carbon bonds is developed. Thus, visible-light driven the building nitrogen-carbon bonds from NH_3 as a feedstock bonded to organic molecule with GluDH and redox

coupling $NADP^+$/ NADPH using photocatalytic dye is accomplished.

The single-electron reduced MV dose not act as co-enzyme for GluDH in the reaction of *L*-glutamate production from 2-oxoglutarate and NH_4^+. To apply GluDH for the visible-light driven redox system with a photocatalytic dye, the redox system of $NADP^+$/NADPH with FNR also is needed to integrate into the system.

The visible-light driven redox system with GluDH and reduction of $NADP^+$ with a system containing an ascorbate as an electron donor, the polyethylene glycol modified chlorophyll-*a* (PEG-Chl-*a*) and FNR as shown in Fig. 42 has been exploited for the production of *L*-glutamate production from 2-oxoglutarate and NH_4^+ for the first time.[198] As mentioned above, $NADP^+$ directly is reduced to NADPH with FNR and PEG-Chl-*a* in this reaction, it is not necessary to add the MV as an electron mediator.

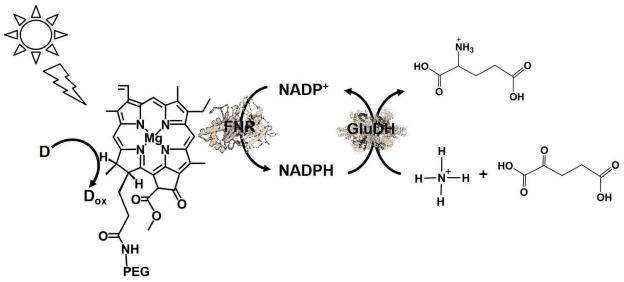

Fig. 42. Scheme of the visible-light driven redox system for *L*-glutamate production from α-oxoglutarate and NH_4^+ and CO_2 consisted of PEG-Chl-*a*, FNR, $NADP^+$, ascorbate and GluDH.

A sample solution is consisted of PEG-Chl-*a* (22.2 μM), ascorbate (8 mM), $NADP^+$ (3.2 mM), α-oxoglutaric acid (8 mM), NH_4Cl (8.0 mM), GluDH (40 units), and FNR (2.5 units) in 10 mL of 100 mM phosphate buffer (pH 7.8). The amount of glutamate is increased with a visible light irradiation time. During irradiation for 44 h, the amount of glutamate produced from α-oxoglutarate and NH_4Cl is determined to be 0.98 mM for which approximately 12 % of α--oxoglutarate (8.0 mM) is converted to glutamate.

Unfortunately, the visible-light driven system the building nitrogen-carbon bonds from NH_3 is only one example of this reaction system, and simple electron mediators like PVs have not been applied yet.

Conclusions and outlook

In this review, focusing on biocatalysts for the visible-light driven CO_2 reduction and utilization systems of a photocatalytic dye and an electron mediator, the following points are outlined.

1) Representative examples of biocatalysts for CO_2 reduction and utilization are introduced.

2) The visible-light driven CO_2 reduction and utilization with a photocatalytic dye and biocatalyst via the $NAD(P)^+$/ NADPH or BP/BP_{red} redox coupling are introduced.

Especially, the visible-light driven CO_2 reduction and utilization with a photocatalytic dye and biocatalyst via the $NAD(P)^+$/ NADPH or BP/BP_{red} redox coupling are described in detail. There is no doubt that it is effective to use the $NAD(P)^+$/ NAD(P)H redox coupling for the visible-light driven CO_2 reduction and utilization with biocatalyst. These systems can be applied to utilization *in vivo* capable of regenerating $NA(P)^+$/NADPH. The affinity between natural co-enzyme, $NAD(P)^+$ or NAD(P)H and biocatalyst does not change, however, biocatalyst catalytic activity cannot be controlled with $NAD(P)^+$/NAD(P)H redox coupling. As the produced $NAD(P)^+$/ NADPH works as an electron donor, in other words, a sacrificial reagent and is consumed, moreover, the $NAD(P)^+$/ NADPH redox coupling is not suitable to use for the visible-light driven CO_2 reduction and utilization with a photocatalytic dye and biocatalyst. Even if the effective $NAD(P)^+$ reduction to NAD(P)H with visible-light driven redox system could be achieved, $NAD(P)^+$ is a very expensive biological reagent. Furthermore, since $NAD(P)^+$ cannot be reduced directly to NAD(P)H with a photocatalytic dye, a second electron mediator such as a rhodium complex or second catalyst such as a FNR is indispensable for the development of visible-light driven CO_2 reduction and utilization. If researchers refer to the contribution to the substantial CO_2 reduction with the visible-light driven redox system of a photocatalytic dye and biocatalyst using use the $NAD(P)^+$/ NAD(P)H redox coupling *in vitro*, the complexity of the system cannot be denied. Unfortunately, it is obvious that the visible-light driven redox system of a photocatalytic dye and biocatalyst using use the $NAD(P)^+$/NAD(P)H redox coupling *in vitro* has its limit unless devising a commercially available biocatalyst and a corresponding co-enzyme. Thus, it is necessary to design and prepare a simple molecule that is easily reduced with a photocatalytic dye and acts as a co-enzyme for biocatalyst. 4,4′- or 2,2′- BPs, that have been widely used as an electron mediator molecule in the visible-light driven redox system, has paid attention, because BPs can be easily chemically modified. By using chemically modified BPs, the catalytic activity of biocatalyst for CO_2 reduction and utilization can be controlled. There are reports that it is better to use natural co-enzyme the $NAD(P)^+$/NAD(P)H redox coupling because BP, especially MV is toxic material.[133] However, this opinion is an irrelevant idea, catalytic activity of commercially available biocatalyst cannot be controlled with $NAD(P)^+$/NAD(P)H redox coupling. Thus, controlling the catalytic activity of biocatalyst with cheap molecules is an important point for the practical application of visible-light driven redox system with a commercially available biocatalyst *in vitro*. By using a single electron mediator based on the simple molecule for visible-light driven CO_2 reduction and utilization with a photocatalytic dye and biocatalyst, the reaction system is simpler than that of system using $NAD(P)^+$/ NAD(P)H redox coupling.

For example, simple device for the visible-light driven CO_2 reduction to formate consisting of a Chl-e_6, a BP with long alkyl chain ($CH_3V(CH_2)_9COOH$) and FDH has been developed as shown in Fig. 43. [199]

By using this device, formate production based on the CO_2 reduction with visible-light irradiation in the presence of a suitable electron donor has been developed. After 3 h visible light irradiation, 2.0 mM formate is produced by using this device.

Of course, BPs are not versatile as an electron mediator for biocatalyst in the light driven redox system with a photocatalytic dye. BPs is used under saturation of inert gas such as nitrogen or argon in the visible-light driven redox system because of deactivation of the single-electron reduced BPs by oxygen. As dissolved oxygen in the sample solution can be removed with CO_2 as an inert gas, MV will be used as an electron mediator of the visible-light driven CO_2 reduction and utilization system using a photocatalytic dye and biocatalyst.

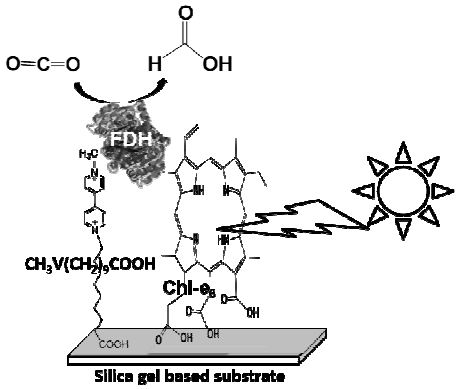

Fig. 43. Device for the visible-light driven CO_2 reduction to formate consisting of a Chl-e_6, a BP with long alkyl chain ($CH_3V(CH_2)_9COOH$) and FDH.

Moreover, most of the systems introduced in this review so far require an electron donor in other words, a sacrificial reagent, and how to use electron sources such as a water is an important factor in the future. There is also a proposal to replace the process involving the sacrificial reagent of the visible-light driven CO_2 reduction system of photocatalytic dye and biocatalyst with a hydrolysis system of saccharide or only saccharide. For example, visible-light driven CO_2 reduction to formate with FDH coupling the glucose oxidation with glucose dehydrogenase (GDH) *Thermoplasma acidophilum* (EC 1.1.1.47) and the reduction of MV by photosensitization of ZnTPPS via the NAD^+/NADH redox cycle has been reported as shown in Fig. 44.[200]

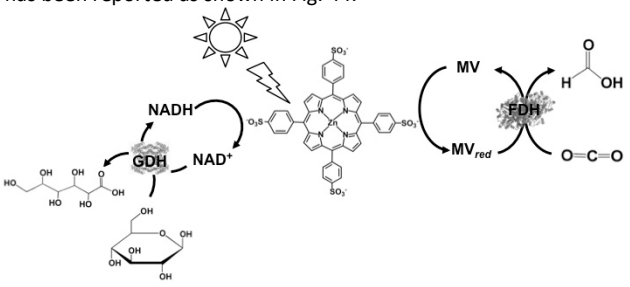

Fig. 44. Scheme of the visible-light driven CO_2 reduction to formate with FDH coupling the glucose oxidation with GDH and the reduction of MV by photosensitization of ZnTPPS via the NAD^+/NADH redox cycle.

As mentioned above, NADH acts as a sacrificial reagent and NAD^+ is consumed in the visible-light driven redox system of a ZnTPPS, MV and FDH. In the system shown in Fig. 43, as NADH is regenerated with GDH, the visible visible-light driven redox system is accomplished without NAD^+ consumption.

Oxygen produced due to water oxidation in the visible-light driven redox system deactivates on a biocatalyst or an electron mediator, so it is necessary to separate the oxygen production system from the CO_2 reduction system. The visible-light driven CO_2 reduction with a photocatalytic dye and a biocatalyst using water as an electron donor also has been reported.[201] The visible-light driven electrochemical biofuel-based cell consisting of the thylakoid membrane of microalgae *Spirulina platensis* immobilized on a TiO_2 layer electrode as a photoanode, a FDH/ $CH_3V(CH_2)_9COOH$ co-immobilized electrode as a cathode, and a CO_2-saturated buffer solution as the redox electrolyte, is developed as shown in Fig. 45. By using this cell, formate and oxygen are produced stoichiometrically with visible light irradiation. Unfortunately, efficiency of CO_2 reduction is still low in this system, but efficient CO_2 reduction system using water as an electron donor will be achieved by a photoanode with effective photocatalytic material such as $BiVO_4$.

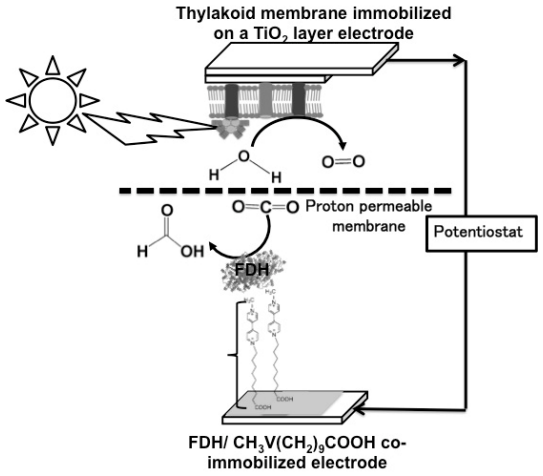

Fig. 45. Device for visible-light driven cell with Thylakoid membrane on TiO_2 layer electrode as an anode and FDH/$CH_3V(CH_2)_9COOH$ co-immobilized electrode as a cathode.

In the future, it is expected that new technologies with biocatalyst will be developed for the effective and practical use for the visible-light driven CO_2 reduction and utilization with the system of a photocatalytic dye, an effective simple and cheap electron mediator and biocatalyst.

Acknowledgements

Our work introduced in this review is partially supported by Precursory Research for Embryonic Science and Technology (PRESTO, Japan Science and Technology Agency JST), Grant-in-Aid for Challenging Exploratory Research (Japan Society for the Promotion of Science) (15K14239), and Grant-in-Aid for Scientific Research on Innovative Areas "Artificial Photosynthesis (2406)" and "Innovations for Light-Energy Conversion (4906)".

Notes and references

1 E.S. Sanz-Pérez, C.R. Murdock, S.A. Didas and C.W. Jones, *Chem. Rev.*, 2016, **116**, 11840.
2 K. Takeuchi, "6th International Conference on Greenhouse Gas Control Technologies "Elsevier, Kyoto **2002**, 849.
3 http://unfccc.int/resource/docs/2015/cop21/eng/l09r01.pdf (ADOPTION OF THE PARIS AGREEMENT)
4 J.R. Darwent, P. Douglas, A. Harriman, G. Porter and M.C. Richoux, *Coord. Chem. Rev.,* 1982, **44**, 93.
5 P.A. Brugger, P. Cuendet and M. Grätzel, *J. Am. Chem. Soc.,* 1981, **103**, 2923.
6 I. Okura, *Coord. Chem. Rev.,* 1985, **68**, 53.
7 I. Okura, *Biochimie,* 1986, **68**, 189.
8 Y. Amao, *Current Nanoscience,* 2008, **4**, 45.
9 Y. Amao and I. Okura, "*Sensitization by Metal Complexes Towards Future Artificial Photosynthesis"* in Photocatalysis, Kodansha Springer, **2002**.
10 A. Harriman, G. Porter and M.-C. Richoux, *J. Chem. Soc., Faraday Trans. 2,* 1981, **77**, 833.
11 I. Okura and N. Kim-Thuuan, *J. Mol. Catal.,* 1979, **6**, 227.
12 I. Okura, M. Takeuchi and N. Kim-Thuuan, *Photochem. Photobiol.,* 1981, **33**, 413.
13 I. Okura, M. Takeuchi, S. Kusunoki and S. Aono, *Inorg. Chim. Acta,* 1982, **63**, 157.
14 I. Okura, N. Kaji, S. Aono, T. Kita and A. Ymada, *Inorg. Chem.,* 1985, **24**, 451.
15 Y. Amao, Y. Tomonou, Y. Ishikawa and I. Okura, *Int. J. Hydrogen Energy*, 2002, **27**, 621.
16 Y. Tomonou and Y. Amao, *Biometals,* 2002, **15**, 391.
17 Y. Tomonou and Y. Amao, *Biometals,* 2003, **16**, 419.
18 N. Sugiyama, M. Toyoda and Y. Amao, *Colloids, Surfaces A: Physicochemical and Engineering Aspecs,* 2006, **284-285**, 384.
19 Y. Fuchino and Y. Amao, *Biophysics*, 2006, **2**, 57.
20 Y. Amao, Y. Maki and Y. Fuchino, *J. Phys. Chem. C,* 2009, **113**, 16811.
21 S. Ishigure, A. Okuda, K. Fujii, Y. Maki, M. Nango and Y. Amao, *Bull. Chem. Soc. Jpn.,* 2009, **82**, 93.
22 C.V. Krishnan, B.S. Brunschwig, C. Creutz and N. Sutin, *J. Am. Chem.Soc.,* 1985, **107**, 2005 (Co).
23 C.Baffert, V. Artero and M. Fontecave, *Inorg. Chem.,* 2007, **46**, 1817.
24 X.L. Hu, B.S. Brunschwig and J.C. Peters, *J. Am. Chem. Soc.,* 2007, **129**, 8988.
25 O. Pantani, E. Anxolabehere-Mallart, A. Aukauloo and P. Millet, *Electrochem. Commun.,* 2007, **9**, 54.
26 P. Du, K. Knowles and R. Eisenberg, *J. Am. Chem. Soc.*, 2008, **130**, 12576.
27 K. Sakai and H. Ozawa, *Coord. Chem. Rev.,* 2007, **251**, 2753.
28 M. Wang, Y. Na, M. Görlov and L. Sun, *Dalton Trans.*, 2009, 6458.
29 K. Sakai, Y. Kizaki, T. Tsubomura and K. Matsumoto, *J. Mol. Catal.* 1993, **79**, 141.
30 H. Ozawa, Y. Yokoyama, M. Haga and K. Sakai, *Dalton Trans.*, 2007, **36**, 1197.
31 H. Ozawa, M. Haga and K. Sakai, *J. Am. Chem. Soc.,* 2006, **128**, 4926.
32 H. Ozawa, M. Kobayashi, B. Balan, S. Masaoka and K. Sakai, *Chem. Asian J.,* 2010, **5**, 1860.
33 S. Masaoka, Y. Mukawa and K. Sakai, *Dalton Trans.*, 2010, **39**, 5868.
34 J. W. Peters, W. N. Lanzilotta, B. J. Lemon and L. C. Seefeldt, *Science*, 1998, **282**, 1853.
35 Y. Nicolet, C. Piras, P. Legrand, C. E. Hatchikian and J. C. Fontecilla-Camps, *Structure*, 1999, **7**, 13.
36 Y. Na, M. Wang, J. Pan, P. Zhang, B. Åkermark and L. Sun, *Inorg. Chem.,* 2008, **47**, 2805.
37 L.-C. Song, M.-Y. Tang, F.-H. Su and Q.-M. Hu, *Angew. Chem., Int. Ed.*, 2006, **45**, 1130.
38 L.-C. Song, M.-Y. Tang, S.-Z. Mei, J.-H. Huang and Q.-M. Hu, *Organometallics*, 2007, **26**, 1575.
39 R. Lomoth and S. Ott, *Dalton Trans.*, 2009, **38**, 9952.
40 D. Streich, Y. Astuti, M. Orlandi, L. Schwartz, R. Lomoth, L. Hammarstrcm and S. Ott, *Chem. Eur. J.,* 2010, **16**, 60.
41 S. Ott, M. Kritikos, B. Åkermark and L. Sun, *Angew. Chem., Int. Ed.*, 2003, **42**, 3285.
42 S. Salyi, M. Kritikos, B. Åkermark and L. Sun, *Chem.–Eur. J.*, 2003, **9**, 557.
43 S. Ott, M. Borgström, M. Kritikos, R. Lomoth, J. Bergquist, B. Åkermark, L. Hammarström and L. Sun, *Inorg. Chem.*, 2004, **43**, 4683.
44 J. Ekström, M. Abrahamsson, C. Olson, J. Bergquist, F. B. Kaynak, L. Eriksson, L. Sun, H.-C. Becker, B. Åkermark, L. Hammarström and S. Ott, *Dalton Trans.*, 2006, **35**, 4599.
45 C. Wombwell, C.A. Caputo and E. Reisner, *Acc. Chem. Res.*, 2015, **48**, 2858.
46 W. Lubitz, H. Ogata, O. Rüdiger and E. Reijerse, *Chem. Rev.,* 2014, **114**, 4081.
47 K.A. Vincent, A. Parkin and F.A. Armstrong, *Chem. Rev.,* 2007, **107**, 4366.
48 S. Yoshizawa and A. Böck, *Biochim. Biophys. Acta,* 2009, **1790**, 1404.
49 C.S.A. Baltazar, M.C. Marques, C.M. Soares, A.M. DeLacey, I.A.C. Pereira and P.M. Matias, *Eur. J. Inorg. Chem.,* 2011, 948.
50 E. Garcin, X. Vernede, E.C. Hatchikian, A. Volbeda, M. Frey and J.C. Fontecilla-Camps, *Structure,* 1999, **7**, 557.
51 F.M.A. Valente, A.S.F. Oliveira, N. Gnadt, I. Pacheco, A.V. Coelho, A.V. Xavier, M. Teixeira, C.M. Soares and I.A. Pereira, *J. Biol. Inorg. Chem.,* 2005, **10**, 667.
52 A. Parkin, G. Goldet, C. Cavazza, J.C. Fontecilla-Camps and F.A. Armstrong, *J. Am. Chem. Soc.,* 2008, **130**, 13410.
53 L. Sun, B. Akermark and S. Ott, *Coord. Chem. Rev.,* 2005, **249**, 1653.
54 A.A. Krasnovski, G.P. Brin and U.V. Nikandrov, *Dokl. Acad. Nauk. SSSR.* 1975, **228**, 1214.
55 J.A.M. Smith and D. Mauzerall, *Photochem. Photobiol.,* 1981, **34**, 407.
56 G. McLendon and D.S. Miller, *J. Chem. Soc., Chem. Commun.*, 1980, 533.
57 I. Okura, M. Takeuchi, S. Kusunoki and S. Aono, *Inorg. Chim. Acta,* 1982, **63**, 157.
58 C.A. Caputo, M.A. Gross, V.W. Lau, C. Cavazza, B. Lotsch and E. Reisner, *Angew. Chem., Int. Ed.,* 2014, **53**, 11538.
59 T. Sakai, D. Mersch and E. Reisner, *Angew. Chem., Int. Ed.,* 2013, **52**, 12313.
60 E. Reisner, J.C. Fontecilla-Camps and F.A. Armstrong, *Chem. Commun.,* 2009, 550–552.
61 E. Reisner, *Eur. J. Inorg. Chem.,* 2011, 1005.
62 C.A. Caputo, L. Wang, R. Beranek and E. Reisner, *Chem. Sci.,* 2015, **6**, 5690.
63 Y. Amao and I. Okura, *J. Mol. Catal. A. Chem.,* 1996, **105**, 125.
64 Y. Amao and I. Okura, *J. Mol. Catal. A. Chem.,* 1995, **103**, 1995 69.
65 Y. Amao, Y. Tomonou and I. Okura, *Solar Energy Materials & Solar Cells,* 2003, **79**, 103.
66 T. Itoh, A. Ishii, Y. Kodera, A. Matsushima, M. Hiroto, H. Nishimura, T. Tsuzuki, T. Kamachi, I. Okura and Y. Inada, *Bioconjugate. Chem.* 1998, **9**, 409.
67 Y. Hori, K. Kikuchi, A. Murata and S. Suzuki, *Chem. Lett.,* 1986, **15**, 897.
68 Y. Hori, A. Murata and R. Takahashi, *J. Chem. Soc., Faraday Trans. I,* 1989, **85**, 2309.
69 J. Yuan, L. Liu, R.R. Guo, S. Zeng, H. Wang and J.X. Lu, *Catalysts,* 2017, **7**, 220.

70 Q. Li, J.J. Fu, W.L. Zhu, Z.Z. Chen, B. Shen, L.H. Wu, Z. Xi, T.Y. Wang, G. Lu and J.J. Zhu, *J. Am. Chem. Soc.,* 2017, 139, 4290.
71 C.H. Lee and M.W. Kanan, *ACS Catal.,* 2015, **5**, 465.
72 X.F. Feng, K.L. Jiang, S.S. Fan and M.W. Kanan, *J. Am. Chem. Soc.,* 2015, **137**, 4606.
73 C.W. Li and M.W. Kanan, *J. Am. Chem. Soc.,* 2012, **134**, 7231.
74 M. Gattrell and N. Gupta, *J. Electroanal. Chem*., 2006, **594**, 1.
75 R. Reske, H. Mistry, F. Behafarid, B.R. Cuenya and P. Strasser, *J. Am. Chem. Soc.,* 2014, **136**, 6978.
76 K.P. Kuhl, E.R. Cave, D.N. Abramc and T.F. Jaramillo, *Energy Environ. Sci.,* 2012, **5**, 7050.
77 Z. Wang, K. Teramura, Z. Huang, S. Hosokawa, Y. Sakata and T. Tanaka, *Catal. Sci. Technol.,* 2016, **6**, 1025.
78 K. Teramura, H. Tatsumi, W. Zheng, S. Hosokawa and T. Tanaka, *Bull. Chem. Soc. Jpn,* 2015, **88**, 431.
79 Z. Wang, K. Teramura, S. Hosokawa and T. Tanaka, *Appl. Catal. B: Environ.,* 2015, **163**, 241.
80 M. Yamamoto, T. Yoshida, N. Yamamoto, T. Nomoto, Y. Yamamoto, S. Yagi and H. Yoshida, *J. Mater. Chem. A*, 2015, **3**, 16810.
81 T. Yoshida, N. Yamamoto, T. Mizutani, M. Yamamoto, S. Ogawa, S. Yagi, H. Nameki and H. Yoshida, *Catal. Today*, 2018, **303**, 320.
82 M. Yamamoto, S. Yagi and T. Yoshida, *Catal. Today*, 2018, **303**, 334.
83 H. Takeda, K. Koike, H. Inoue and O. Ishitani, *J. Am. Chem. Soc.,* 2008, **130**, 2023.
84 B. Gholamkhass, H. Mametuska, K. Koike, T. Tanabe, M. Furue and O. Ishitani, *Inorg. Chem.,* 2005*,* **44,** 2326.
85 K. Kiyosawa, N. Shiraishi, T. Shimada, D. Masui, H. Tachibana, S. Takagi, O. Ishitani, D.A. Tryk and H. Inoue, *J. Phys. Chem. C,* 2009, **113**, 11667.
86 H. Kumagai, G. Sahara, K. Maeda, M. Higashi, R. Abe and O. Ishitani, *Chem. Sci.,* 2017, **8**, 4242.
87 Y. Tamaki and O. Ishitani, *ACS Catal.*, 2017, **7**, 3394.
88 H. Takeda, C. Cometto, O. Ishitani and M. Robert, *ACS Catal.,* 2017, **7**, 70.
89 G. Sahara, H. Kumagai, K. Maeda, N. Kaeffer, V. Artero, M. Higashi, R. Abe and O. Ishitani, *J. Am. Chem. Soc,.* 2016, **138,** 14152.
90 J. Rohacova and O. Ishitani, *Chem. Sci.,* 2016, **7**, 6728.
91 M. Deguchi, S. Yotsuhashi, Y. Yamada and K. Ohkawa, *Adv. Cond. Mat. Phys.,* 2015, Article ID 537860.
92 H. Rao, L. C. Schmidt, J. Bonin and M. Robert, *Nature*, 2017, **548**, 74.
93 S. Aoi, K. Mase, K. Ohkubo, T. Suenobu and S. Fukuzumi, *ACS Energy Lett.,* 2017, **2**, 532.
94 K. Faber, *Biotransformations in Organic Chemistry* 3rd edn. ed., Springer, Berlin, 201 (1997).
95 Y. Amao, *ChemCatChem*, 2011, **3**, 458.
96 C.L. Bird and A.T. Kuhn, *Chem. Soc. Rev.,* 1981, **10**, 49.
97 O. Meyer and H.G. Schlegel, *J. Bacteriol.,* 1980, **141**, 74
98 S.W. Ragsdale, J.E. Clark, L.G. Ljungdahl, L.L. Lundie and H.L. Drake, *J. Biol. Chem.,* 1983, **258**, 2364.
99 T.I. Doukov, T.M. Iverson, J. Seravalli, S.W. Ragsdale and C.L. Drennan, *Science,* 2002, **298**, 567.
100 C.L. Drennan, J. Heo, M.D. Sintchak, E. Schreiter and P.W. Ludden, *Proc. Natl. Acad. Sci.,* 2001, **98**, 11973.
101 H. Dobbek, V. Svetlitchnyi, L. Gremer, R. Huber and O. Meyer, *Science,* 2001, **293**, 1281.
102 D.C. Davison, *Biochem. J.,* 1950, **49**, 520.
103 J.R. Quayle, *Methods Enzymol.,* 1966, **9**, 360.
104 D.R. Jollie and J.D. Lipscomb, *J. Biol. Chem.,* 1991, **266**, 21853.
105 E. Racker, *J. Biol. Chem*., 1950, **184**, 313.
106 B.A. Manjasetty, J. Powlowski and A. Vrielink, *Proc. Natl. Acad. Sci.,* 2003, **100**, 6992
107 S. Harada, *The Anthropological Society of Nippon,* 1991, **99**, 123
108 Y. Lei, P.D. Pawelek and J. Powlowski, *Biochemistry,* 2008, **47**, 6870.
109 E.G. Brandt, M. Hellgren, T. Brinck, T. Bergman and O. Edholm, *Phys. Chem. Chem. Phys*., 2009, **11**, 975.
110 P. Zucca, M. Littarru, A. Rescigno and E. Sanjust, *Biosci. Biotech. Bioch*., 2009, **73**, 1224
111 R. Obert and B. C. Dave, *J. Am. Chem. Soc.,* 1999, **121***,* 12192.
112 B. El-Zahab, D. Donnelly and P. Wang, *Biotech. Bioeng.,* 2007, **99***,* 508.
113 M. Ando, T. Yoshimoto, S. Ogushi, K. Rikitake, S. Shibata and D. Tsuru, *J. Biochem.,* 1979, **85**, 1165.
114 W. Hohnloser, B. Osswald and F. Lingens, *Z. Physiol. Chem.,* 1980, **361**, 1763
115 I. Harary, S.R. Korey and S. Ochoa, *J. Biol. Chem.,* 1953, **203**, 595
116 S. Ochoa, A.H. Mehler and A. Kornberg, *J. Biol. Chem.,* 1948, **74**, 979.
117 W.J. Rutter and H.A. Lardy, *J. Biol. Chem.,* 1958, **233**, 374.
118 D.B. Cherbavaz, M.E. Lee, R.M. Stroud and D.E. Koshland, *J. Mol. Biol.,* 2000, **295**, 377.
119 H. Tarhonskaya, A.M. Rydzik, I.K.H. Leung, N.D. Loik, M.C. Chan, A. Kawamura, J.S. McCullagh, T.D.W. Claridge, E. Flashman and C.J. Schofield, *Nature Commun*., 2014, **5**, 3423.
120 F. J. Corpas, J. B. Barroso, L. M. Sandalio, J. M. Palma, J.A. Lupiáñez and L. A. del Río. *Plant Physiology*, 1999, **121**, 921
121 Y.Ohno, T. Nakamori, H. Zheng and S. Suye, *Biosci. Biotech. Bioch.,* 2008, **72**, 1278.
122 H. Zheng, T. Nakamori, and S. Suye, *J. Biosci. Bioeng.,* 2009, **107**, 16.
123 K. Hironaka, S. Fukuzumi and T. Tanaka, *J. Chem. Soc., Perkin Trans. 2,* 1984, 1705.
124 H. Wu, C. Tian, X. Song, C. Liu, D. Yang and Z. Jiang, *Green Chem.,* 2013, **15**,1773.
125 F. Hollmann, I. W. C. E. Arends and K. Buehler, *ChemCatChem,* 2010, **2**, 762.
126 F. Hollmann, B. Witholt and A. Schmid, *J. Mol. Catal. B: Enzym.,* 2002, **19–20**, 167.
127 D.E. Torres Pazmino, M. Winkler, A. Glieder and M.W. Fraaije, *J. Biotechnol.,* 2010, **146**, 9.
128 Y. Maenaka, T. Suenobu, and S. Fukuzumi, *J. Am. Chem. Soc.,* 2012, **134**, 367.
129 Z. Y. Jiang, C. Q. Lü and H. Wu, *Ind. Eng. Chem. Res.,* 2005, **44**, 4165.
130 Q. Shi, D. Yang, Z. Y. Jiang and J. Li, *J. Mol. Catal. B: Enzym.,* 2006, **43**, 44.
131 C. B. Park, S. H. Lee, E. Subramanian, B. B. Kale, S. M. Lee and J. O. Baeg, *Chem. Commun.,* 2008, 5423.
132 R. K. Yadav, J.-O. Baeg, G. H. Oh, N.-J. Park, K.-J. Kong, J. Kim, D. W. Hwang and S. K. Biswas, *J. Am. Chem. Soc.,* 2012, **134**, 11455.
133 R. K. Yadav, G. H. Oh, N.-J. Park, A. Kumar, K.-J. Kong and J.-O. Baeg, *J. Am. Chem. Soc.,* 2014, **136**, 16728.
134 R. K. Yadav, J.-O. Baeg, A. Kumar, K.-J. Kong, G. H. Oh and N.-J. Park, *J. Mater. Chem. A,* 2014, **2**, 5068.
135 M. Ihara, Y. Kawano, M. Urabe and A. Okabe, *PLoS One*, 2013, **8**, e71581.
136 K. J. Shah and T. Imae, *J. Mater. Chem. A,* 2017, **5**, 9691.
137 C. Drewke and M. Ciriacy, *Biochim. Biophy.s Acta,* 1988, **950**, 54.
138 H. Wang, D. Xiao, C. Zhou, L. Wang, L. Wu, Y. Lu, Q. Xiang, K. Zhao, X. Li and M. Ma, *Appl. Microbiol. Biotechnol.,* 2017, **101**, 4507.
139 X. Wang, C.J. Mann, Y. Bai, L. Ni and H. Weiner, *J. Bacteriol.,* 1998, **180**, 822.

140 S. Ogushi, M. Ando and D. Tsuru, *Agric. Biol. Chem.,* 1984, **48**, 597.
141 A. Andreadeli, D. Platis, V. Tishkov, V. Popov and N.E. Labrou, *FEBS J.,* 2008, **275**, 3859.
142 T. Schmidt, C. Michalik, M. Zavrel, A. Spiess, W. Marquardt and M. B. Ansorge-Schumacher, *Biotechnol. Prog.,* 2010, **26**, 73.
143 Y. Amao, *Chem. Lett.*, 2017, **46**, 780.
144 D. Mandler and I. Willner, *J. Chem. Soc., Perkin Trans. 2*, 1988, 997.
145 I. Willner and D. Mandler, *J. Am. Chem. Soc.*, 1989, **111**, 1330.
146 I. Willner, N. Lapidot, A. Riklin, R. Kasher, E. Zahavy and E. Katz, *J. Am. Chem. Soc.*, 1994, **116,** 1428.
147 I. Willner and N. Lapidot, *J. Am. Chem. Soc.*, 1990, **112**, 6438.
148 M. Kodaka and Y. Kubota, *J. Chem. Soc., Perkin Trans. 2*, 1999, 891.
149 Y. Amao, R. Abe and S. Shiotani, *J. Photochem. Photobiol. A. Chem.,* 2015, **313**, 149.
150 S. Ikeyama, R. Abe, S. Shiotani and Y. Amao, *Chem. Lett.*, 2016, **45**, 979.
151 S. Ikeyama, R. Abe, S. Shiotani and Y. Amao, *Bull. Chem. Soc. Jpn.,* accepted. doi:10.1246/bcsj.20180013.
152 R. Miyatani and Y. Amao, *Biotechnol. Lett*., 2002, **24,** 1931.
153 R. Miyatani and Y. Amao, *J. Mol. Catal. B. Enzym.*, 2004, **27**, 121.
154 R. Miyatani and Y. Amao, *J. Jpn. Petrol. Inst*., 2004, **47**, 27.
155 S. Ikeyama and Y. Amao, *Sustainable Energy Fuels*, 2017, **1**, 1730.
156 S. Ikeyama and Y. Amao, *Photochem. Photobiol. Sci.,* 2018, **17**, 60.
157 S. Ikeyama, T. Katagiri and Y. Amao, *J. Photochem. Photobiol. A. Chem.*, 2018, **358**, 362.
158 S. Ikeyama and Y. Amao, *Chem. Lett.*, 2016, **45**, 1259.
159 S. Ikeyama and Y. Amao, *ChemCatChem*, 2017, **9**, 833.
160 I. Tsujisho, M. Toyoda, and Y. Amao, *Catal. Commun.*, 2006, **7**, 173.
161 Y. Amao and T. Watanabe, *Chem. Lett.*, 2004, **33**,1544.
162 Y. Amao and T. Watanabe, *Appl. Catal. B: Environ.,* 2009, **86**,109.
163 Y. Amao and R. Kataoka, *Catal. Today,* 2018, **307**, 243.
164 S. Kuwabata, K. Nishida, R. Tsuda, H. Inoue and H. Yoneyama, *J. Elcectrochem. Soc.,*1994, **141**, 1488.
165 M. G. van Kleef, J. Jongejan, and J. Duine, in *PQQ and Quinoproteins*, J. A. Jongejan and J. A. Duine, eds., p. 217, Springer Netherlands, (1989).
166 S. Itoh, M. Kinugawa, N. Mita, and Y. Ohshiro, *J. Chem. Soc., Chem. Commun.*, 1989, **11**, 694 .
167 E. Katz, D. D. Schlereth and H.-L. Schmidt, *J. Electroanal. Chem.*, 1994, **367**, 59.
168 E. Katz, D. D. Schlereth, H.-L. Schmidt and A. J. J. Olsthoorn, *J. Electroanal. Chem.*, 1994, **368**, 165.
169 I. Emahi, M. Mitchell and D.A. Baum, *J. Elcectrochem. Soc.,* 2017, **164**, 3097.
170 T. W. Woolerton, S. Sheard, E. Reisner, E. Pierce, S.W. Ragsdale and F. A. Armstrong, *J. Am. Chem. Soc.,* 2010, **132**, 2132.
171 T. W. Woolerton, S. Sheard, E. Pierce, S. W. Ragsdale and F. A. Armstrong, *Energy Environ. Sci.,* 2011, **4**, 2393.
172 Y. S. Chaudhary, T. W. Woolerton, C. S. Allen, J. H. Warner, E. Pierce, S.W. Ragsdale and F. A. Armstrong, *Chem. Commun.,* 2012, **48**, 58.
173 A. Bachmeier, V. C. C. Wang, T. W. Woolerton, S. Bell, J. C. Fontecilla-Camps, M. Can, S. W. Ragsdale, Y. S. Chaudhary and F. A. Armstrong, *J. Am. Chem. Soc.,* 2013, **135**, 15026.
174 Y. Amao, *SPR Photochemistry*, 2018, **45**, 163.
175 L. Willner, D. Mandler and A. Riklin, *J. Chem. Soc. Chem. Commun.,* 1986, 1022.
176 T. Omura, E. Sanders and R.W. Estabrook, *Arch. Biochem. Biophys.,* 1966, **117**, 660.
177 M. Shin, K. Tagawa and D.I. Arno, *Biochem. Z,* 1963, **338**, 84.
178 J. M. Berg, J. L. Tymoczko and L. Stryer, Biochemistry (6th ed.). New York: W.H. Freeman (2007).
179 A. Aliverti, V. Pandini, A. Pennati, M. de Rosa and G. Zanetti, *Arch Biochem. Biophys.* 2008, **474**, 283.
180 J.P. Benz, M. Lintala, J. Soll, P. Mulo and B. Bölter, *Trends Plant Sci.,* 2010, **15**, 608.
181 H. Inoue, M. Yamachika and H. Yoneyama, *J. Chem.. Soc. Faraday Trans.,* 1992, **88**, 2215.
182 Y. Amao and M. Ishikawa, *J. Jpn. Petrol. Inst*., 2007, **50**, 272.
183 Y. Amao and M. Ishikawa, *Catal. Commun.*, 2007, **8**, 423.
184 T. Itoh, H. Asada, K. Tobioka, Y. Kodera, A. Matsushima, M. Hiroto, H., Nishimura, T. Kamachi, I. Okura and Y. Inada, *Bioconjugate Chem*., 2000, **11**, 8.
185 H. Kamogawa and S. Sato, *Bull. Chem. Soc. Jpn.,* 1991, **64**, 321.
186 T. Katagiri, S. Ikeyama and Y. Amao, *J. Photochem. Photobiol. A. Chem.*, 2018, **358**, 368.
187 Y. Amao, S. Ikeyama, T. Katagiri and K. Fujita, *Faraday Discuss.,* 2017, **198**, 73.
188 T. Katagiri, K. Fujita, S. Ikeyama and Y. Amao, *Pure Appl. Chem.,* in submitted.
189 H. Inoue, Y. Kubo and H. Yoneyama, *J. Chem. Soc., Faraday Trans.,* 1991, **87**, 553.
190 Y. Amao, N. Shuto and H. Iwakuni, *Appl. Catal. B: Environ.,* 2016, **180**, 403.
191 P. D. Watson, *Ind. Eng. Chem.,* 1948, **40**, 1393.
192 C. J. Valvona, H. L. Fillmore, P. B. Nunn and G. J. Pilkington, *Brain Pathology,* 2016, **26**, 3.
193 J.R. Pineda, R. Callender and S.D. Schwartz *Biophys. J.*, 2007, **93**, 1474.
194 R. Miyatani and Y. Amao, *Photochem. Photobiol. Sci.,* 2004, **3**, 681.
195 J.W. Coulton and M. Kapoor, *Can. J. Microbiol.,* 1973, **19**, 427.
196 S. Grisolia, C.L. Quijada and M. Fernandez, *Biochim. Biophys. Acta,* 1964, **81**,61.
197 I. Shiio and H. Ozaki, *J. Biochem.,* 1970, **68**, 633.
198 H. Asada, T. Itoh, Y. Kodera, A. Matsushima, M. Hiroto, H. Nishimura and Y. Inada, *Biotechnol. Bioeng.,* 2001, **76**, 86.
199 Y. Amao, N. Shuto, K. Furuno, A. Obata, Y. Fuchino, K. Uemura, T. Kajino, T. Sekito, S. Iwai, Y. Miyamoto and M. Matsuda, *Faraday Discuss,.* 2012, **155,** 289.
200 Y. Amao, S. Takahara and Y. Sakai, *Int. J. Hydro. Energ.,* 2014, **39**, 20771.
201 Y. Amao, M. Fujimura, M. Miyazaki, M. Nakamura, A. Tadokoro and N. Shuto, *New J. Chem.,* 2018, **42**, 9269.

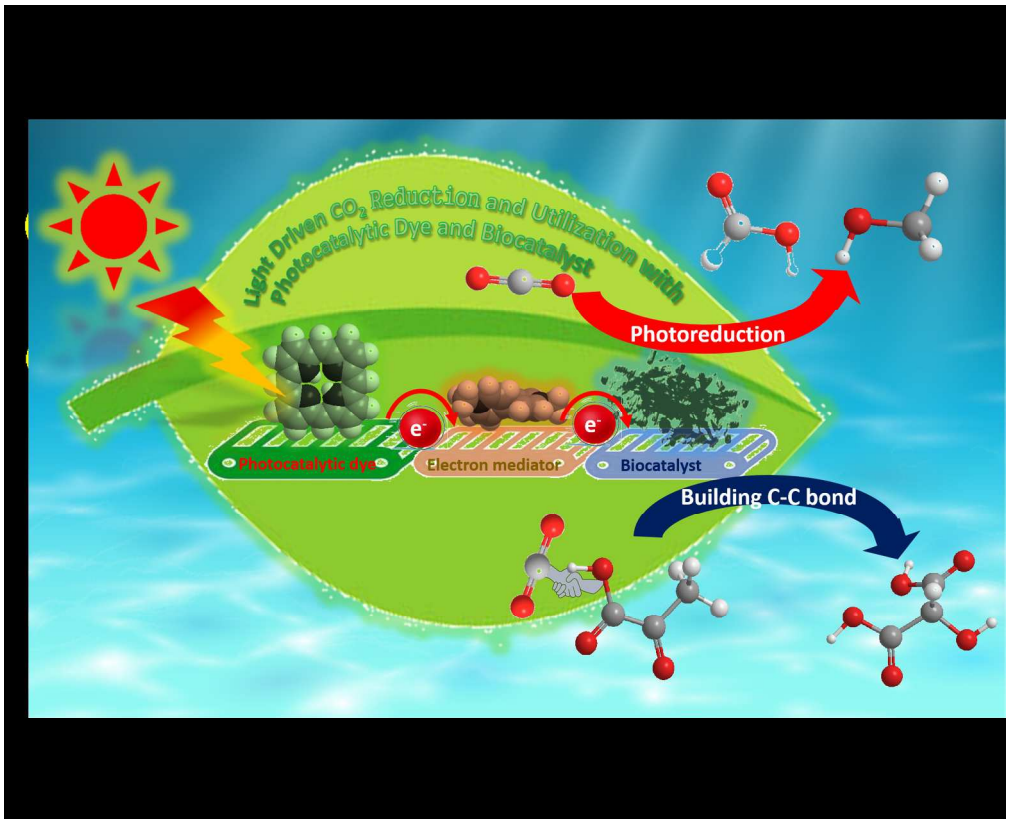

353x286mm (150 x 150 DPI)